Prins Maurits Laboratorium TNO

TNO-Defensieonderzoek

TD

AD-A263 372

TNO Prins Maurits Laboratory

TNO Defence Research

TNO-report
PML 1992-52

January 1993

Copy no.: ...

DISTRIBUTION STATEMENT A
Approved for public release;
Distribution Unlimited

Validation of the internal blast response model DAMINEX with the Finite Element Method
Progress report 1. Demonstration of the capabilities of the finite element code ABAQUS

APR 23 1993

Author(s):

R.J.M. van Amelsfort
R.M.M. van Wees

DO-assignment no.

A88/KM/419

Classification

Report:

ONGERUBRICEERD

Title:

ONGERUBRICEERD

Summary:

ONGERUBRICEERD

Annex(es):

ONGERUBRICEERD

Number of copies:

25

Number of pages:
(incl. annex(es), excl. distr. list and RDP)

67

Number of Annexes:

2

The classification designation:

ONGERUBRICEERD

is equivalent to:

UNCLASSIFIED

All information which is classified according to Dutch regulations shall be treated by the recipient in the same way as classified information of corresponding value in his own country.
No part of this information may be disclosed to any party.

Summary

At the request of the Royal Netherlands Navy (RNLN), numerical calculations on blast-loaded ship bulk-heads were performed with the finite element code ABAQUS. These calculations are a first phase in a more extended investigation to validate and improve a simple structural response model, DAMINEX, for these panels. In this first phase, it will be demonstrated that ABAQUS is able to perform this type of calculation. This is done by simulating an ideally suited experiment: a prototype ship panel, loaded by a simulated nuclear blast. In this experiment, performed by the Canadian Defence Research Establishment Suffield, load and response are carefully measured and material properties are well analysed. Simulation results obtained with another finite element code, ADINA, are also available in the literature. The calculated ABAQUS results correspond closely with the measured results and with the ADINA results.
A second ABAQUS simulation was performed of a live-firing experiment in a decommisioned RNLN frigate. In the latter case, load, response and boundary conditions are not as well defined as in the first case. It was demonstrated that even in this situation it is possible to obtain reasonable results.
So ABAQUS will be a powerful tool evaluating and improving the DAMINEX model.

Samenvatting

In opdracht van de Koninklijke Marine (KM) zijn numerieke berekeningen aan door blast belaste scheepsschotten uitgevoerd met het eindige elementen programma ABAQUS. Deze berekeningen vormen de eerste fase van een meer uitgebreid onderzoek wat als doel heeft het valideren en verbeteren van een eenvoudig structurele respons model DAMINEX voor dit soort panelen. In deze eerste fase wordt gedemonstreerd dat ABAQUS in staat is dit type berekeningen te verrichten. Dit wordt gedaan door de simulatie van een experiment dat hier ideaal geschikt voor is: een prototype van een scheepspaneel, belast door een nagebootste nucleaire blast. De belastingen en de respons zijn nauwkeurig gemeten in dit experiment en tevens zijn de materiaaleigenschappen geanalyseerd door het Canadeese Defence Research Establishment Suffield. Simulatieresultaten verkregen met ADINA, een ander eindige elementen programma, zijn eveneens beschikbaar in de literatuur. De door ABAQUS berekende resultaten blijken dicht bij de gemeten en bij de door ADINA berekende resultaten te liggen.
Een tweede ABAQUS simulatie is gemaakt van een praktijkproef in een van de sterkte afgevoerd KM fregat. In dit geval waren de belasting, respons en randvoorwaarden niet zo goed bekend als in het vorige experiment. Het wordt aangetoond dat zelfs in dit geval het mogelijk is om redelijke resultaten te behalen.
Dus zal ABAQUS een krachtig instrument vormen om het DAMINEX model te evalueren en te verbeteren.

CONTENTS

1 INTRODUCTION

At the TNO Prins Maurits Laboratory (PML), an internal blast model, named DAMINEX, is under development. This model calculates the response of a ship's construction and the damage development due to an internally exploding warhead. The model is being developed at the request of the Royal Netherlands Navy, under assignment number A88/KM/419.

One important module of DAMINEX is the structural response module, STURES. This module calculates the response of bulkheads due to the pressure loading of an explosion. Practical application of the model needs knowledge of the conditions for which the model gives reliable results. This can be determined by verifying of the validity of the various assumptions and simplifications made in the model under several circumstances. For this purpose, analytical calculations as well as experiments, like the Roofdier experiments, are necessary.

The present investigation is aimed at validating and improving the response module of DAMINEX by means of analytical calculations. This can be achieved by comparing the results of this module with the results of finite element calculations. Numerical simulations with the finite element method can be very useful, and have the advantage of being relatively quick and inexpensive compared to experiments. At PML the finite element code ABAQUS is available and will be used in this investigation. In addition to the comparisons, the strain distribution in the bulkheads will be investigated.

Another important item to be investigated is how the response model can be improved, because some parameters are used whose values cannot be predicted accurately from theoretical considerations. For instance, the deformation of a panel will lie between those with fully clamped boundaries and those with simply-supported boundaries. With the finite element method, the value of parameters used in the STURES module can be calculated, because detailed information of the response can be obtained. Another advantage of finite element calculations is the information which cannot be calculated otherwise: for instance, the strain distribution in a panel can be calculated. This is of great importance, because this strain is important for the remaining deformation capacity of a panel.

The investigation is divided into four phases [van Wees, 1991]. In the first phase of this investigation, two experiments on blast-loaded stiffened ship panels will be analysed with ABAQUS, and the results compared to the results of the experiments. The purpose of this phase is to demonstrate that the ABAQUS code is able to perform this kind of calculation. The second phase compares the responses calculated by DAMINEX and ABAQUS. In the third phase, the stiffness of the supports of the bulkheads will be determined, while in the fourth phase a full three-dimensional ABAQUS calculation will be made.

This report describes the first phase of the investigation: it will be demonstrated that ABAQUS is able to provide good results for this kind of problem. The reason for this is that finite element calculations have been known to give erroneous results in some cases. The causes for these errors are many. Some are caused by errors in the finite element code, others are caused because the problems themselves were ill-conditioned. But most of the errors are caused by the analyst. Modelling mistakes can be made. Some modelling errors, like typing errors, are obvious, but others can be very subtle. For example, the element type can be ill-suited for the problem, or the mesh size, time-step size or tolerances can be chosen too large. Modelling always means schematizing the problem to some degree. Large errors, or even completely meaningless results, can be obtained when important features are neglected in the model.

Most of these errors can be prevented. Errors in the finite element code itself can be minimized by choosing a code which is thoroughly checked both during the development and in practice. ABAQUS meets this requirement. Its developers apply rigourous quality assurance rules, and the thousands of users detect the errors that have slipped through. When the analyst is well trained in the finite element method, modelling errors will be few. Detecting modelling mistakes requires that the analyst has a healthy mistrust in the calculation results and uses adequate quality assurance methods [Zins, 1990]. It is also very important that the analyst has a good physical understanding of the problem. This ensures that no important features are left out of the schematization.

But all these precaution methods do not provide an absolute guarantee that the finite element code and the analyst will be able to produce a good result for a given problem. The ultimate test is to compare the calculated results to the results of a carefully prepared experiment. This is exactly what will be done in this investigation: two experiments on blast-loaded stiffened ship panels will be analysed with ABAQUS, and the results compared to the results of the experiments.

The first experiment is one that is ideally suited to calculate with the finite element method: a prototype ship panel, loaded by a simulated nuclear blast. Everything is carefully controlled, the load and response are exactly measured, the material analysed. The calculation results here should be very close to the experimental results.

The second experiment is a live-firing in a decommisioned ship. Conditions here were much more difficult, with the result that the load, response and boundary conditions are not precisely known. In addition, the finite element calculation will be made with a fairly simple model and without optimization of the input parameters. Naturally, the calculation results in the second case will differ more from the experimental results than in the first case, but this case should demonstrate that it is possible to obtain reasonable results even when the situation is more difficult.

2 RESPONSE CALCULATION OF DRES EXPERIMENT

2.1 Introduction

The main purpose of the calculations described here is to determine the capability of the finite element program ABAQUS to perform response calculations of blast-loaded structures. If ABAQUS is able to perform these calculations, the response model of DAMINEX can be verified in a following stage, with the aid of these theoretical references and the experimentally obtained results.
An experiment performed by the Canadian Defence Research Establishment, Suffield (DRES) during the US Defense Nuclear Agency's event MINOR SCALE in June 1985 was chosen in which a ship panel was loaded by a shock wave [Houlston, 1988]. In this experiment, all relevant phenomena such as membrane action, dynamic response and the influence of stiffeners are present, and the load and response are known accurately. This experiment was analyzed with the finite element code ADINA and the results of this calculation were very close to the results observed experimentally [Houlston, 1988].

2.2 Description of input data

The input is made as close as possible to the input used for the ADINA calculation. Because of symmetry considerations, the calculation can be limited to one quarter of the panel. In addition, the length over height ratio and the stiffeners will make it likely that the panel will respond like a one-way panel instead of a two-way panel. This makes it possible to reduce the model further to just one quarter of the centre panel segment, as illustrated in Figure 1 [Houlston, 1988].

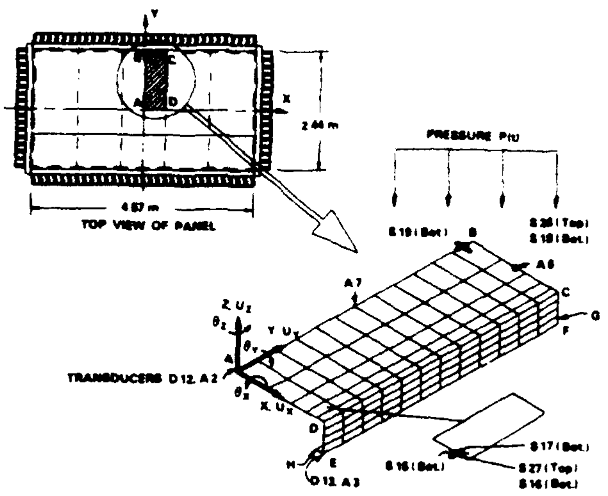

Figure 1 Finite element model of panel section ABCD and beam half section [Houlston, 1988]

The boundary conditions conform [Houlston, 1988] as well: symmetry conditions along the lines AB and HEDH ($U_y = \theta_x = \theta_z = 0$), symmetry conditions along the area EDCF ($U_x = \theta_y = \theta_z = 0$) and fully fixed conditions along the line GFCB ($U_x = U_y = U_z = \theta_x = \theta_y = \theta_z = 0$). The dimensions are 1.22 x 0.457 m^2 (12 x 5 elements with thickness 6.35 mm) for the panel, 1.22 x 0.152 m^2 (12 x 4 elements with thickness 3.5 mm) for the web and 1.22 x 0.038 m^2 (12 x 1 elements with thickness 8.5 mm) for the flange. The thickness of the web is half the thickness of a 152 x 76 T-profile (long stalk T-bar), the thickness of the flange is estimated from the drawing. Figure 2 gives a view of this model with the matching element and node numbers.

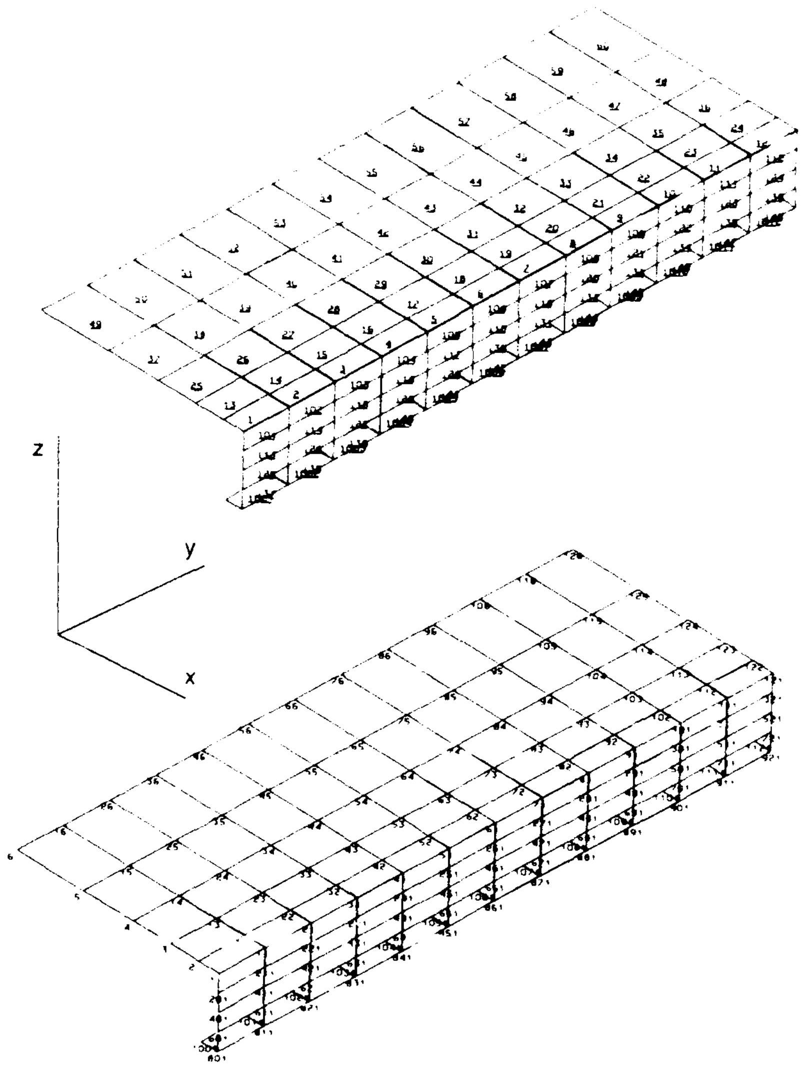

Figure 2 Finite element model of one quarter of the centre panel with the matching element and node numbers

A 4-node quadrilateral shell element with material data conforming to [Houlston, 1988] is chosen. The supplied load is according to the average pressure-time behaviour, as measured in the DRES experiment and given in Figure 3. The full details of this calculation are given in Annex 1.

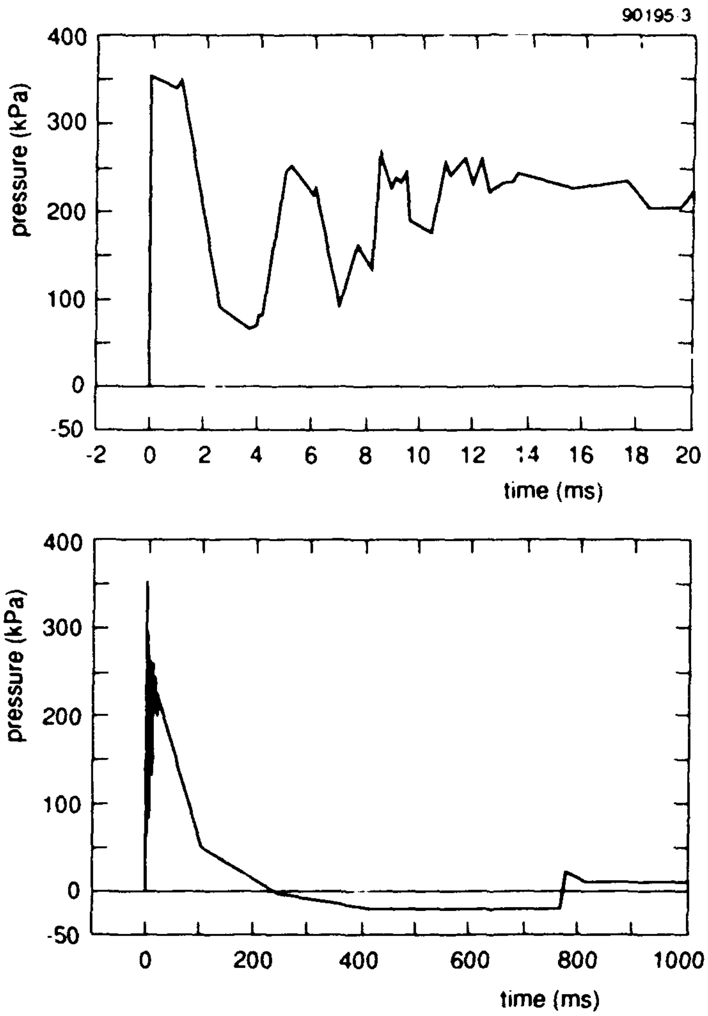

Figure 3 Applied pressure load for the ship panel at two different time scales

The ABAQUS calculation was performed with non-linear geometry, a dynamic stress/displacement analysis with the help of direct integration and a uniformily distributed load according to Figure 3 as surface pressure on the panel.

3 Results of ABAQUS calculation

The results of the ABAQUS run with these input data are presented in a similar way as in [Houlston, 1988]. The calculations show that the panel deforms plastically under the blast load. After the passage of the shock wave, it vibrates around its deformed shape.
Figure 4 gives an impression of the shape of the panel after 10 ms. It also shows the Von Mises stresses. The panel yields in the red coloured areas.

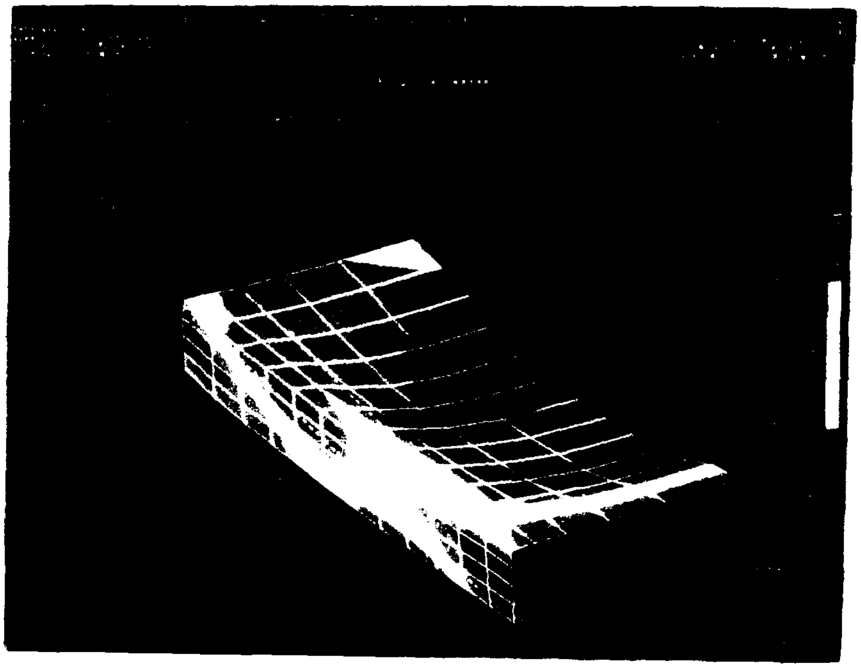

Figure 4 Panel shape and Von Mises stresses after 10 ms

The results of the calculation are summarized in Table 1. It gives a review of the ultimate values of accelerations, displacements and velocities, as calculated with ABAQUS.

Table 1 Ultimate values of accelerations, displacements and velocities calculated with ABAQUS

	Maximum (after ms) Panel centre	Maximum (after ms) Beam mid-span	Minimum (after ms) Panel centre	Minimum (after ms) Beam mid-span
Acceleration (m/s^2)	21500 (7.6 ms)	8026 (6.7 ms)	?	?
Displacement (mm)	52 (17.5 ms)	34 (19 ms)	?	?
Velocity (m/s)	10.6 (8.7 ms)	3.3 (1.9 ms)	-14.7 (2.6 ms)	-8.0 (4.4 ms)

Figure 5 presents the deflection of the centre of the panel and in the beam mid-span, calculated with ABAQUS. It is clear that the centre of the panel is more deflected than the stiffened edge. For comparison, the results of the experiment and the ADINA and ABAQUS calculations are given in Figures 6a and 6b. The figures show that both the ADINA and the ABAQUS calculation predict deflections that lie very close to the experimentally measured deflections. Both calculations show markedly smoother curves than the measurements. This is due to the time-step size used in the numerical integration, which filters out the higher harmonics while leaving the lower frequency vibrations of the panel unaffected. Thus, only the overall behaviour is computed. The figure also shows differences between the two calculated results. They show the same oscillations, but with a different amplitude and a small time shift. This time shift indicates that the two calculations did not use the same time-step size. This implies that some of the rapid load oscillations (see Figure 3) were computed differently, which explains the differences in amplitude of the results.

Annex 1 presents more results and comparisons; among other things displacements, velocities, accelerations and stresses.

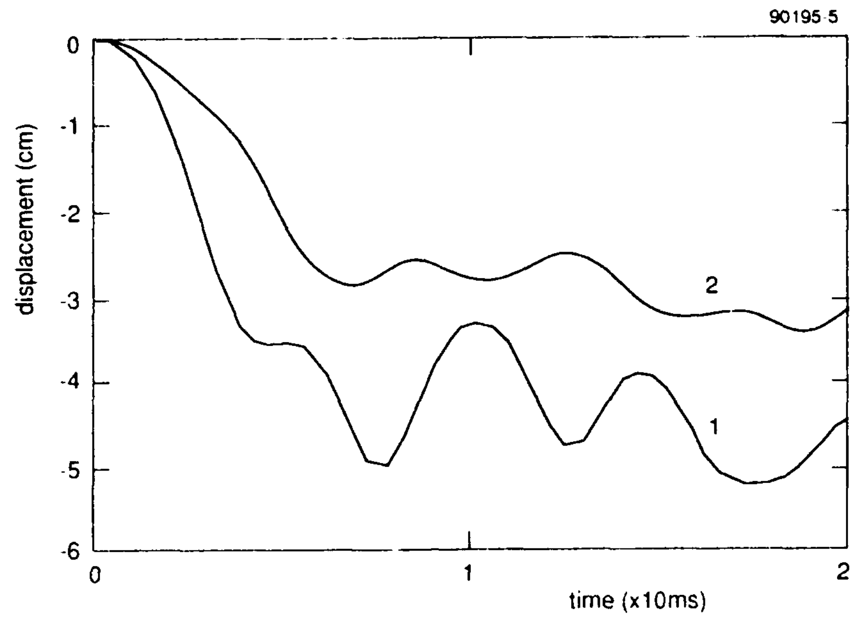

Figure 5 Displacements in the nodes 6 (line 1, panel centre) and 801 (line 2, beam mid-span), calculated with ABAQUS

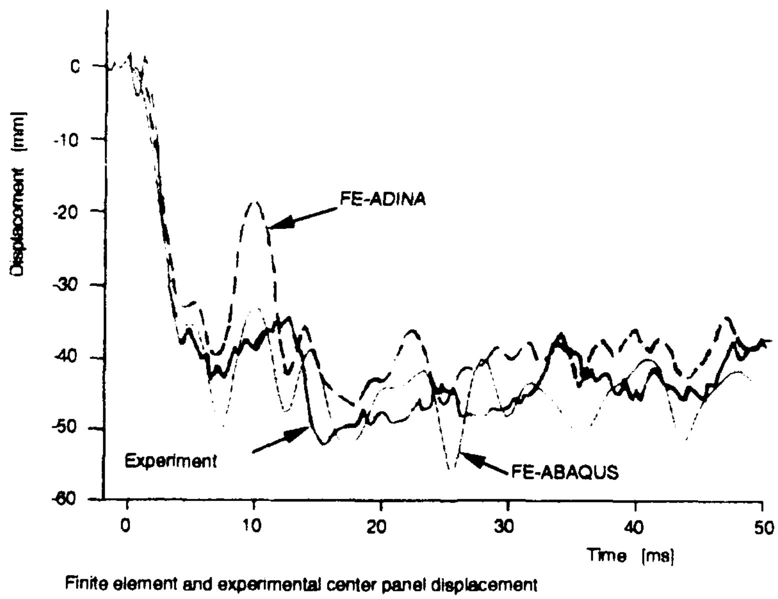

Figure 6a Finite element and experimental centre panel displacement [Houlston, 1988]

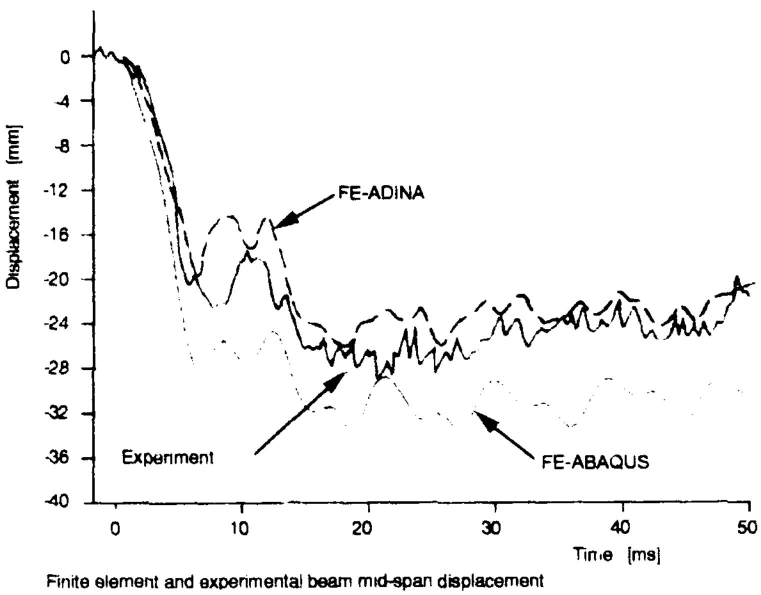

Figure 6b *Finite element and experimental* beam mid-span displacement [Houlston, 1988]

2.4 Comparison with experiment and ADINA calculation

The figures given in Annex 1 can be compared directly with the figures given in [Houlston, 1988]. All the results are essentially the same as those from the ADINA calculations, which in their turn are close to the experimental results. Especially the displacements and the accelerations compare well. The computed strains appear to be relatively sensitive to small changes in the computation. As shown in the tables in Annex 1, they show the largest discrepencies between the two computed results and the experiments.

By and large, the results only differ in detail, such as a slightly greater or smaller magnitude or a small time shift. This is probably due to the choice of the time-step. The time-step size used in the ADINA calculation is too large to follow the acceleration history in all details, as can be seen in Figures 9 and 11 of [Houlston, 1988]. This causes some random discrepencies in the derived parameters, such as the displacement or the strain. The actual time-step size used in the ADINA calculation is not known, neither is the exact flange thickness as used by ADINA. This size was not mentioned in [Houlston, 1988]. However, the results are already close to the ADINA results and to the experimental results. This shows that ABAQUS, with its features like non-linear, dynamic, plastic and membrane behaviour, is able to simulate all of the important characteristics of a blast-loaded stiffened panel, as demonstrated in Figures 6a and 6b.

3 RESPONSE CALCULATION OF ROOFDIER EXPERIMENT

3.1 Introduction

The previous chapter demonstrated that ABAQUS is capable of performing calculations on blast-loaded panels. To demonstrate that useful results can also be obtained in less ideal situations, one of the 'Roofdier' trials was simulated with ABAQUS. The aim is to obtain reasonable results, even if the load and boundary conditions are not known exactly. An experiment with 3 kg centrally detonated TNT in the forward sleeping compartment of a 'Roofdier' class frigate was chosen [Van de Kasteele, Verhagen, 1989]. The reason for this choice is that many parameters were measured in this experiment.
The response of one of the bulkheads of this compartment to the shock pressures and to the quasi-static pressure from the explosion is calculated. Just as in the previous chapter, only a small part of the bulkhead needs to be modelled, because of symmetry.
Instead of directly performing the calculation, first some preliminary calculations were made. The main reason for this approach was to determine some parameters that have to be used in the calculation, such as the mesh size, the time-step size and the numerical tolerances. It is also a good way to spot any errors. Because the preliminary calculations include static calculations, they provide some additional information about the response of the bulkhead as well. More details about this approach are given in [Van Wees, 1991].
The final calculation tries to mimic reality closely, while at the same time using a fairly simple model. More detailed calculations of the experiment are planned in later phases of this project. The most important schematizations are that the influence of adjoining bulkheads is ignored, that the blast pressure is assumed to be equally distributed, and that only a part of the bulkhead is modelled.

3.2 Description of input data

3.2.1 Geometry

The dimensions of the bulkhead (BHD 23) are: average length: 8.0 m, average height: 2.25 m [Sharp, 1951]. The plate thickness is 6.34 mm. The plate is stiffened with T-stiffeners (Figure 7).

Figure 7 View of the bulkhead in the 'ROOFDIER' experiments

Just like in the calculation of the DRES experiment, only a part of the bulkhead is modelled. The main consideration for doing so is efficiency. By choosing to model the part of the bulkhead where the blast load reaches its average value, we believe it will be possible to obtain a reasonably good result at low computational costs. Keeping this cost down is important because it is planned to use the same model many times in the later phases of the project. We believe the results will be reasonably good because since the length over height ratio of bulkhead is large, it will act like a beam clamped between the two decks. Also, the pressure differences that will be present are assumed to be small. Therefore, only a quarter of the part between two stiffeners, and half the stiffener needs to be modelled.

The plate was modelled with 10x20 shell elements (ABAQUS element type S4R, with 5 section points). It was calculated that this number of elements is necessary to obtain a result that lies within 5 % of the result that would be obtained with an infinite amount of elements. Details about this calculation method can be found in [Van Wees, 1988].

The web of the stiffener was modelled with 8 layers of shell elements (ABAQUS element type S4R, with 3 section points), while the flange was modelled with 1 shell element (ABAQUS element type S4R, with 5 section points). Because the stiffener is not welded to the deck, no elements are used in this region. Figure 8 gives a schematization of the connection of stiffener and deck, while Figure 9 presents a plot of the mesh. Full details of the model are given in Annex 2.

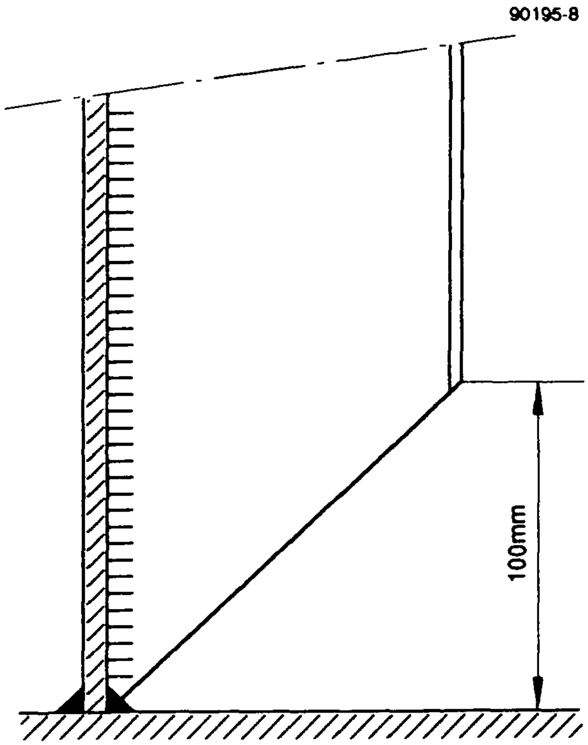

Figure 8 Connection of stiffener and ship deck

It is yet unclear how great the influence of the compliance of the adjacent bulkheads will be on the response. This is one of the points that will be investigated in the later phases of the project. At this moment, the assumption is made that the boundary conditions can be schematized as fully fixed boundaries along the bottom edge (elements 101 to 110) and symmetry boundaries along the two vertical edges and the top edge. This will lead to a stiffer behaviour of the bulkhead than in reality, and therefore in smaller deflections.

3.2.2 Material

The steel of the plate and the stiffeners were modelled as an ideal elastic-plastic material using Von Mises' yield criterion. The yield strength was taken as 275 MPa, in accordance with tests performed on the steel of the ships [v/d Brand and Muller, 1987]. Strain-rate sensitivity of the yield stress was included in the material model. For this, the Cowper-Symonds model was used (see Annex 2).

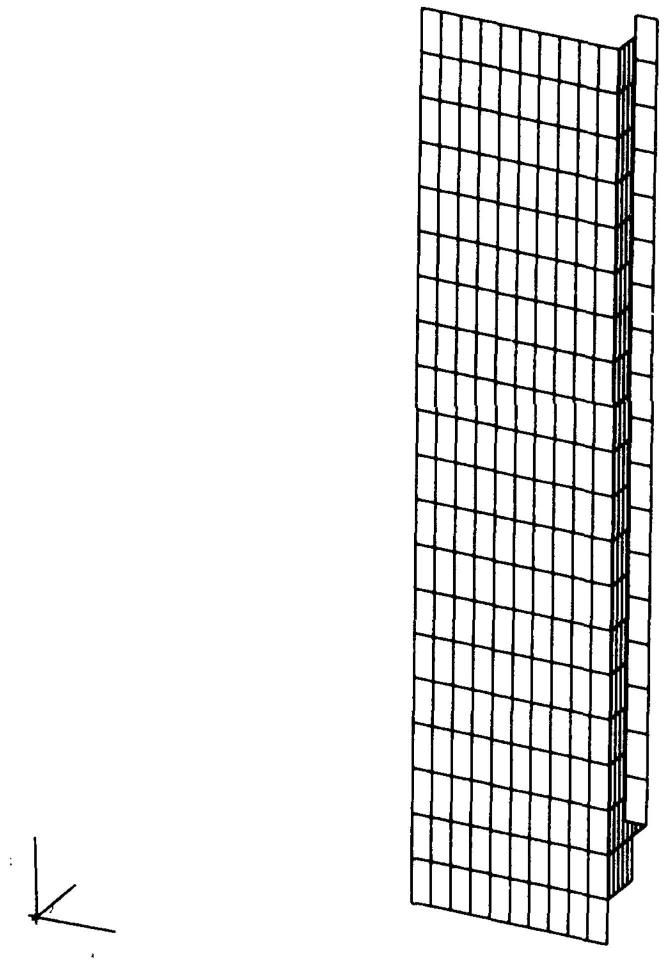

Figure 9 Mesh of a part of the bulkhead

3.2.3 Load

In the primary phase, the load on the bulkhead consisted of the shock wave from the detonation, followed by several reflections. This phase is followed by the quasi-static pressure build-up and its gradual decay.

This complicated load has been schematized. Because only a small part of the bulkhead is considered, it is assumed that the pressure is equally distributed over the plate. The pressure history is simplified by considering only the first shock wave, one reflection and the quasi-static pressure (Figure 10). The magnitude and duration of the pressures were taken from measurements [Van de Kasteele, Verhagen, 1989] and modelled accordingly as free air blast curves as used in DAMINEX. Both shock waves were modelled with the relation:

$$p(t) = p_r \frac{1(t-t_a)}{t_p} \cdot e^{\frac{-\alpha(t-t_a)}{t_p}}$$

where:

p	reflected pressure	(Pa)
t	time	(s)
t_a	arrival time of shock wave	(s)
p_r	peak pressure	(Pa)
t_p	duration of shock wave	(s)
α	decay constant	(-)

The values used are given in Table 2.

Table 2 Parameters used to model the shock waves

	t_a (ms)	p_r (kPa)	t_p (ms)	α (-)
First shock wave	0	700	1.9	1.76
Second shock wave	2.3	350	1.9	1.76

The quasi-static pressure was modelled as a triangular wave, starting at 2.8 ms, reaching its maximum pressure of 120 kPa at 27.8 ms, and decaying to zero at 2500 ms (Figure 10).

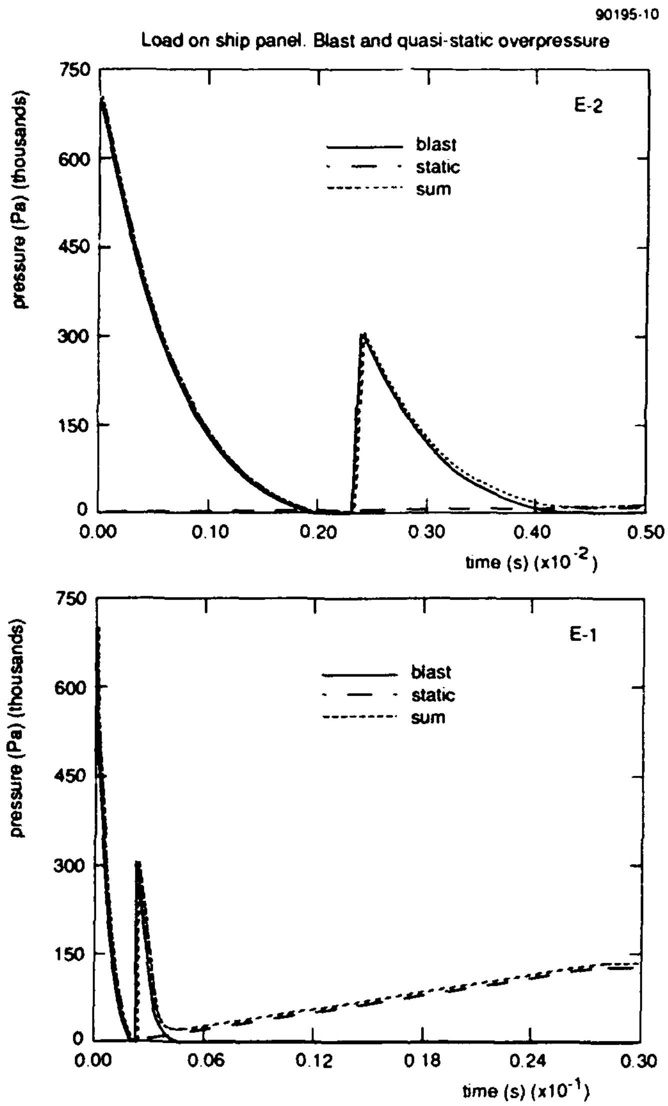

Figure 10 Pressure-load history at different time-scales

3.2.4 Calculation method

The calculation was made with a transient dynamic analysis. Non-linear geometric effects were included. The Hilber-Hughes a-method was used for the implicit time integration, with the numerical damping ratio a set to -0.05 [ABAQUS Users' Manual, 1989]. The calculations were made up to a time of 3000 ms.

3.3 Results of preliminary calculations

Although the preliminary calculations were principally made to determine parameters such as mesh size, time-step size and tolerances, some of the results are of interest in their own right. These are the static load-deflection curve and the static strain distribution.

3.3.1 Static load-deflection curve

A static deformation calculation was made using the same model as described above, with the exception of the dynamic calculation method. Figure 11 presents the load-deflection curve that resulted from this calculation. The model used a non-linear material and included geometric non-linearities. The deflection used is the deflection under the stiffener (the deflection in the middle of the plate is very nearly the same).

It becomes clear that the plate yields after 10 mm deflection at a pressure of 30 kPa. Then a phase of combined elastic and plastic deformation begins. The increasing stiffness in this phase is partly due to membrane effects. After 60 mm, all the elastic capacity is used, and all subsequent deformation is purely plastic. The plate is fully loaded by membrane stresses in this phase.

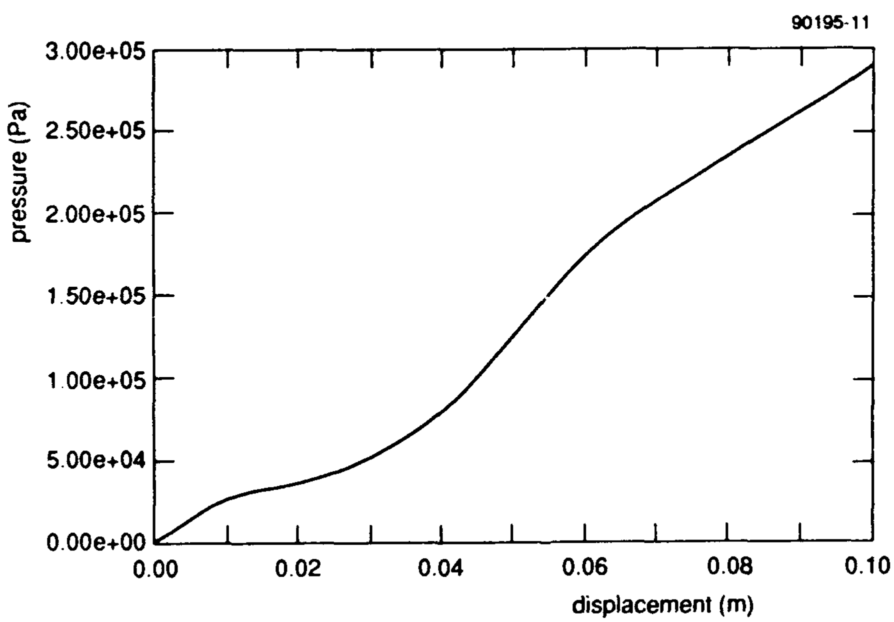

Figure 11 Static load-deflection curve

3.3.2 Static strain distribution

It is assumed in the single degree of freedom method that the strain distribution under dynamic loading is approximately the same as under a static load. This assumption can be verified by comparing the strain distribution for the static fully non-linear case with the dynamic strain distribution.

Figure 12 shows the Von Mises strain for a load of 200 kPa. The maximum deflection is 65 mm. The strain in the plate is below the yield strain in most parts. Only the clamped edge of the plate deforms plastically. The difference in deflection between the stiffened edge and the centre of the panel is minimal.

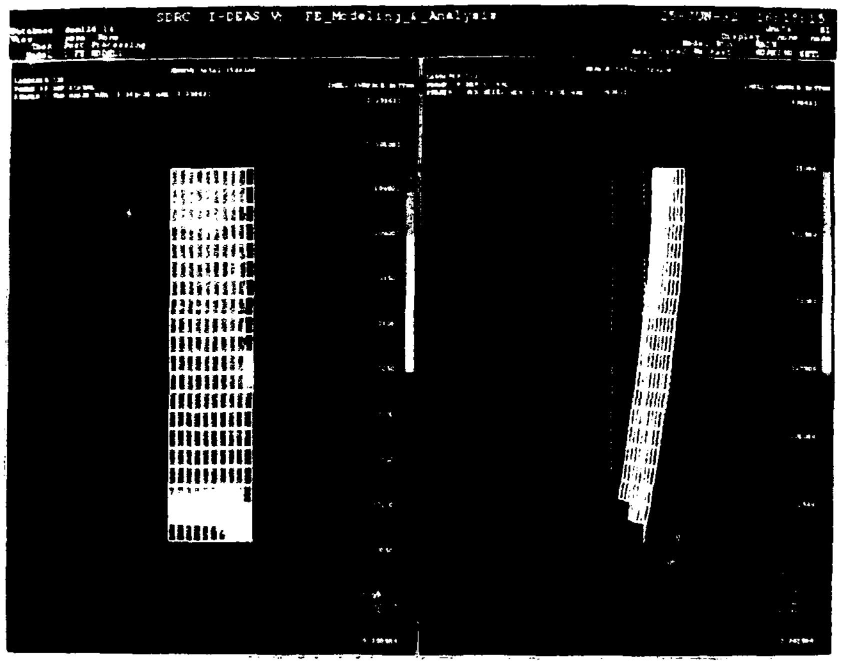

Figure 12 Static strain distribution

3.4 Results of main problem calculation

With the same model as described above, dynamic deformation calculations were made. Again, a number of versions were run, one using a linear material and ignoring geometric non-linearities, one using a linear material but including geometric non-linearities, and finally one using a non-linear material and including geometric non-linearities. The latter was also performed with strain-rate dependent yield stress. This calculation is the most realistic one and its results will be compared with experimental measurements in the next chapter.
The calculated vertical displacement history of the top right (beam mid-span) and top left (panel centre) nodes (node numbers 2111 and 2101 respectively) for the latter approach are given in Figure 13. This figure shows that the panel reaches its maximum deflection after 3 vibrations, with most deformation in the first vibration. There is almost no difference in deflection between the beam mid-span and the panel centre. The beam mid-span is deflected slightly more, which is contrary to expectation.

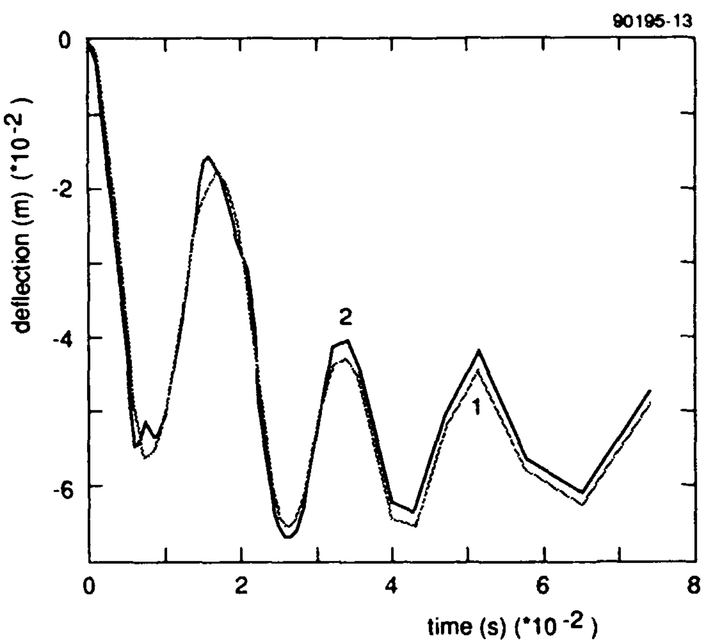

Figure 13 Displacement of nodes 2111 (beam mid-span, line 2) and 2101 (panel centre, line 1), obtained with a dynamic ABAQUS calculation, using a non-linear material and including geometric non-linearities and strain-rate dependency of the yield stress

Also the calculated kinetic energy, elastic strain energy and energy dissipated in plastic deformation summed on the entire model is given (Figure 14). The figure shows that plastic deformation (line 3) takes place in short bursts during the first 65 ms. 60 % of the plastic deformation occurs during the first vibration. The kinetic energy (line 1) is rapidly damped away. This is mainly due to the plastic deformation, but a small fraction is due to damping which is included in the numerical integration method. This graduately damps the vibrations of the panel, which show up as vibrations in the elastic strain energy (line 2) of the model. The maximum elastic strain energy is about 700 J, much more than the elastic strain energy for the static load when the deflection is 50 mm (about 200 J). This indicates that the yield stress is raised due to the strain-rate effect. The energy dissipated in plastic deformation is about 700 J, only 3.5 times the maximum static elastic strain energy. This means that the panel is not severly loaded by the explosion.
Notice that the time-scale for the figures given here differs from the time-scale for the figures given in Annex 2. The calculated Von Mises stresses and strains at a number of times are also given in Annex 2.

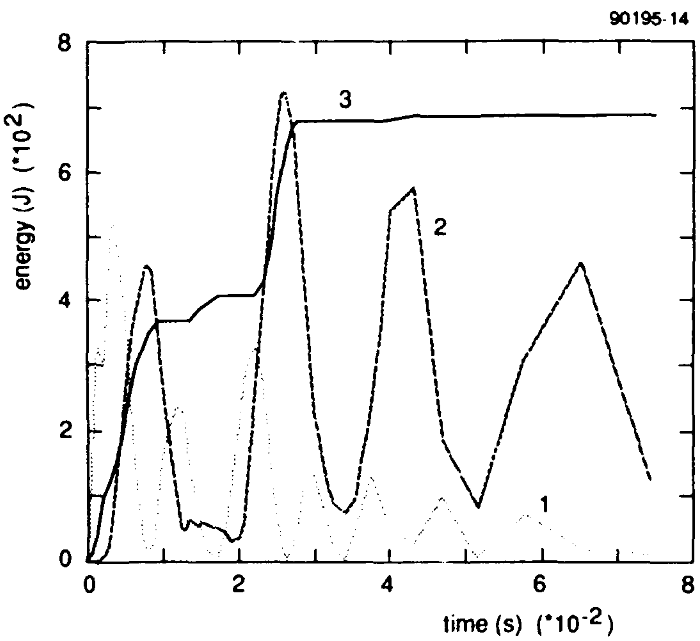

Figure 14 Energies summed on the entire model, obtained with a dynamic ABAQUS calculation, using a non-linear material and geometric non-linearities and including strain-rate dependency of the yield stress

3.5 Comparison with experiment

For the comparison with the Roofdier experiment, only the calculation with a non-linear material behaviour and including geometric non-linearities and strain-rate dependency of the yield stress is considered. The calculated final deflection of both top right and top left nodes is about 37 mm, as shown in Figure 15. The influence of adjacent bulkheads above and below the deforming bulkhead is not considered in the calculation, so the bulkhead will behave stiffer and the calculated response will be smaller. The experimentally found deflection was about 60 mm, but this value was roughly determined, while the deflection before the experiment was not established. So, the experimentally found deflection can be taken as 60 ± 15 mm.

Figure 16 gives the total energies, as mentioned in section 3.4, during a longer time period (3 s). The elastic strain energy (line 2) decays as the quasi-static pressure diminishes, but it is apparent that considerable residual stresses remain. The residual elastic strain energy is about 50 J, which is about half of the elastic strain energy for a static load that gives a deflection of 37 mm.

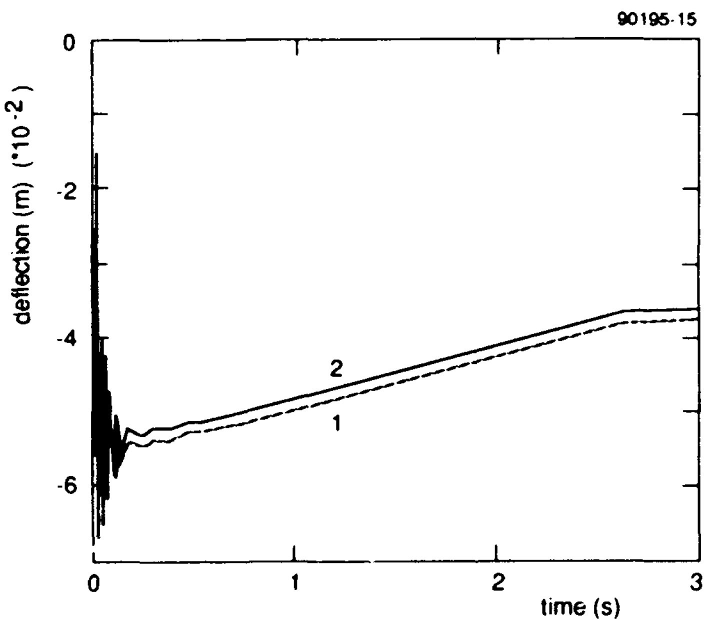

Figure 15 Calculated final deflection of top right node (beam mid-span, line 2) and top left node (panel centre, line 1)

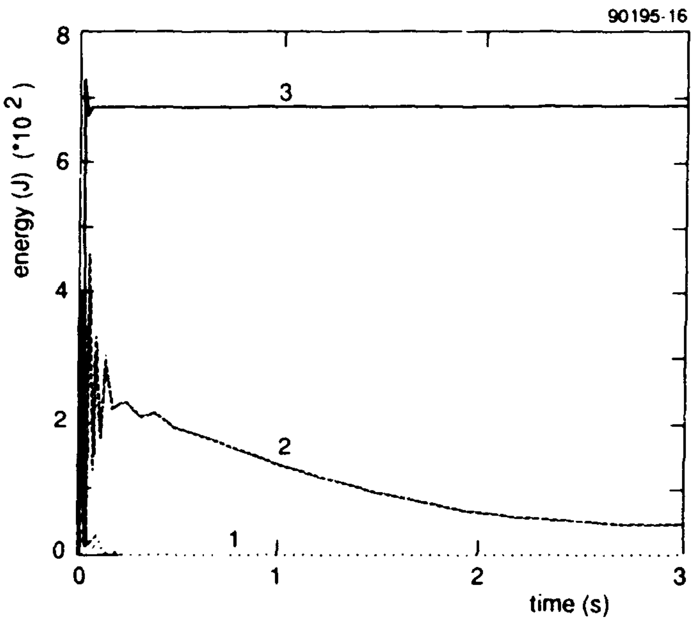

Figure 16 Calculated total energies in time. Line 1 is kinetic energy, line 2 is elastic strain energy and line 3 is energy dissipated in plastic deformation

A comparison between the strain measurements as given in [v.d. Kasteele and Verhagen 1991] and the strain as calculated by ABAQUS is made. Experimental strain gauge positions which are comparable with model positions are given in Table 3. The strain measurements were performed on a 300 ms and a 3 s time base. Annex 2 gives both the measured [v.d. Kasteele and Verhagen, 1991] and calculated strain histories.

Table 3 Experimental strain gauge positions compared with model positions

Gauge number	Position	Model element number
S4*, S5, S [illegible]*, S15	80 mm from stiffener, along model bottom edge	106, 206[1]
S6*, S7	260 mm from stiffener, along model top edge	2001
S11	centre stiffener, along model top edge	2010
S12*	260 mm from stiffener, along model bottom edge	201
S16	back of stiffener, along model bottom edge	210

* Gauge inside experiment compartment
1 Gauge lies on the border between these two elements

As can be seen from these figures, it is difficult to compare the results obtained with the experimental results. For efficiency, a greater time-step than that necessary to handle all vibrations in the plate has been used after the shock phase, and numerical damping appears. Because the plate behaves linear elastic at that time, this greater time-step is allowable. For efficiency as well, a rather simple model has been used. The most important schematizations are the ignoring of the influence of adjacent bulkheads, the assumption of equally distributed applied blast pressure and the modelling of only a part of the bulkhead. With these simplifications it is not surprising that the strain calculation and the measured strain signals are only roughly comparable. Also, the calculation of the DRES experiment showed that strain signals are more sensitive to small disturbances than deflection or acceleration signals.

Although both applied load and panel geometry are not quite equal as in the experiment, the order of magnitude of the calculated strain-time behaviour is the same as experimentally measured (Figure 17). The agreement is best during the first vibrations, when small time-steps are used in the numerical integration. Note that the strain momentarily exceeds the static yield strain (1300 μstrain) in the experimentally measured signal. Because the strain rate is high, the material does not actually yield.

An overview of all calculated and measured final strains is given in Table 4.

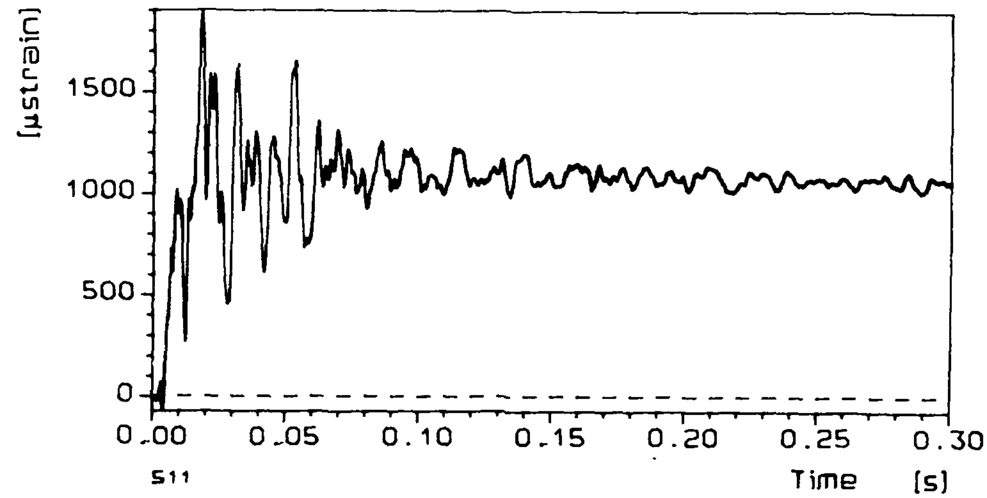

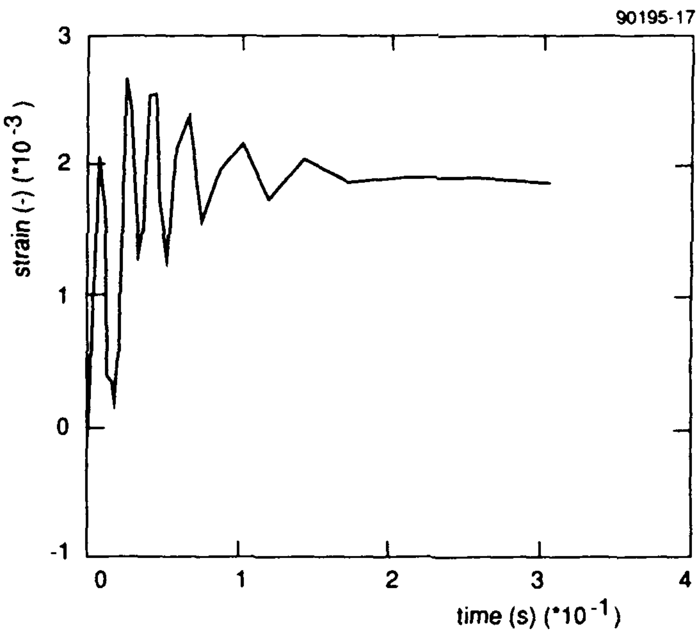

Figure 17 Strain histories during 300 ms at centre of stiffener along model top edge S11 measured and line 1 calculated at position outside experiment compartment

Table 4 Calculated and measured final strains

Position µstrain	Measured µstrain	Calculated	Figure
80 mm from stiffener, along model bottom edge	600 / 100[2]	7100 / -700[1]	B9
	-600 / 500[*2]	295 / 1025[*1]	B9
260 mm from stiffener, along model top edge	1500[*]	790[*]	B10
	-200	115	B10
centre of stiffener, along model top edge	600[*]	2400[*]	B11
260 mm from stiffener, along model bottom edge	-700	-770	B12
back of stiffener, along model bottom edge	700[*]	-1120 / 4130[*1]	B13

* Values for positions outside experiment compartment, or values for positions inside experiment compartment

1 Gauge lies on the border between two elements

2 Two gauges, one near the floor, one near the ceiling

These results show that both the measured and computed strains are sensitive to the exact location of the gauge, especially when it lies near the clamped edge of the panel. This is easily understood by looking at Figures B14 or B15. These show a strong strain gradient near the edge. This gradient is partly real and partly a numerical artefact. Overall, the agreement is reasonable.

4 CONCLUSIONS

It has been demonstrated that ABAQUS is very capable of simulating a stiffened panel loaded by a blast wave. Already the first attempt to simulate the DRES experiment gave results very similar to those of the experiments and the ADINA calculations. The ABAQUS results approximate the experimental results even better than ADINA in several cases. Especially the deflection and acceleration signals agree well. The strain signals appear to be more sensitive to small disturbances, but they agree with each other as well.
The results of the ABAQUS calculations and the ROOFDIER experimental results, concerning final deflection and strain histories, are reasonably comparable. They are mostly in the same order of magnitude and lie within the experimental scattering as demonstrated in Annex 2. The differences between the calculated results and the measurements are larger than with the DRES experiment. This is due to the fact that the load on the panel and its boundary conditions are not exactly known and that some schematizations were made in the finite element model.

The DAMINEX model is based on structural mechanics, which implies that the bulkheads are schematized, the loads are exactly known, and the boundary conditions are well defined. Thus, the situation is much more comparable to the ideal situation of the DRES experiment than to the ROOFDIER experiment. Therefore, the final conclusion is that ABAQUS will be a powerful tool for evaluating and improving the DAMINEX model.

5 AUTHENTICATION

Rolf van Wees

R.J.M. van Amelsfort
(Author)

R.M.M. van Wees
(Author/Project leader)

6 REFERENCES

ABAQUS Users' Manual, Version 4-8
Hibbitt, Karlsson & Sorensen, Inc.
Providence, Rhode Island, 1989

Brand, B.E.H.C. van de; Muller, M.K.
Qualification record plate material Code H dek SPT88A
Metaalinstituut TNO, Apeldoorn, 7 December 1987

British Standard Long Stalk T-bars, 4A:1934, Suppl.No.1 (1989)

Houlston, R
A nonlinear dynamic response analysis of a ship-stiffened panel subjected to an air-blast explosion
1988 ASME PVP Conference, Pittsburg, Pennsylvania, June 19-23

Kasteele, R. van de; Verhagen, Th.L.A.
Instrumented experiments on board of frigate "WOLF"
Wolf II: Measurement results of the 3 kg TNT experiment in the crew front sleeping compartment
TNO Prins Maurits Laboratory, PML 1992-11, Rijswijk, 1992

Sharp, George G. Inc., dwg. no. v-2275 s11-5-3, N.Y., 1951
PCE 1604 class. Transverse bhds. 18, 23, 8, 32

Wees, R.M.M. van
Study plan 'Validatie en verbetering van het responsmodel van DAMINEX m.b.v. ABAQUS'
TNO Prins Maurits Laboratorium, Rijswijk, 18 januari 1991

Wees, R.M.M. van
Berekeningsmethoden voor de beschermingskunde
1 Lineair-elastische responsberekeningen met ABAQUS
(Calculation Methods for Military Engineering
1 Linear Elastic Response Calculations with ABAQUS)
TNO Prins Maurits Laboratory, PML 1988-81, Rijswijk, May 1988

Wees, R.M.M. van
Calculation Methods for Military Engineering
2 Nonlinear Response Calculations with ABAQUS
TNO Prins Maurits Laboratory, PML 1991-18, Rijswijk, April 1991

Zins, J.W.
Survey result on finite element model quality control
Finite Element News, No. 1, pp. 40-43, Feb. 1990

ANNEX 1 INPUT DATA AND RESULTS OF DRES SIMULATION

Input data

The quadrilateral shell element (S4R was chosen). This element has 4 nodes; it was developed for large displacements, material plasticity, small element strains, non-linear analysis and spatially constant loads [ABAQUS Users' Manual, 1989]. The number of section points of each element is set to 9 for the panel and the flange, and 5 for the web.

Overview of the material data conform to [Houlston, 1988] used for the ABAQUS simulation:

mass density	:	7770 kg/m^3
Young's modulus	:	206.9 GPa
Poisson's ratio	:	0.3
yield stress panel	:	375 MPa
web	:	370 MPa
flange	:	340 MPa
tangent modulus panel	:	1225 MPa
web	:	1300 MPa
flange	:	1450 MPa

The stress-strain curve is approximated bilinearly (Figure A1). The linear elastic behaviour is isotropic and the elastic-plastic behaviour, where the yield stress only depends on the plastic strain, contains isotropic hardening.

The boundary conditions conform to [Houlston, 1988] as well (see Figure A2 for numbering):

- symmetry conditions along the line with nodes 1, 16,..., 126 ($U_x=\theta_y=\theta_z=0$)
- symmetry conditions along the line with nodes 1001, 801, 601,...1, 2,..., 6 ($U_y=\theta_x=\theta_z=0$)
- symmetry conditions along the area with elements 101 up to and including 148 ($U_x=\theta_y=\theta_z=0$)
- fully fixed conditions along the line with nodes 1121, 921, 721, ..., 121, 122, ..., 126 ($Ux = Uy = Uz = \theta x = \theta y = \theta z = 0$)

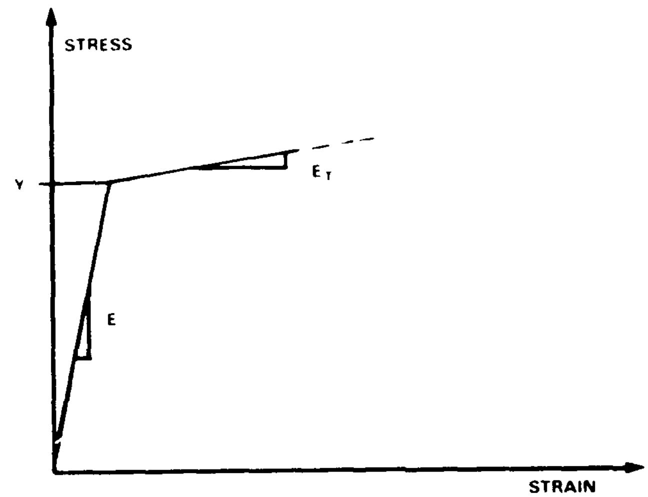

Figure A1 Illustration of a bilinear approximation of the stress-strain curve

For the ABAQUS calculation, the following parameters are set:

recommended first time increment 1 μs;

maximum time increment 0.5 ms;

half-step residual tolerance to be used with the automatic time stepping HAFTOL = 200000;

numerical (artificial) damping control parameter ALPHA = -0.05;

force equilibrium tolerance needed for implicit integration PTOL = 1000.

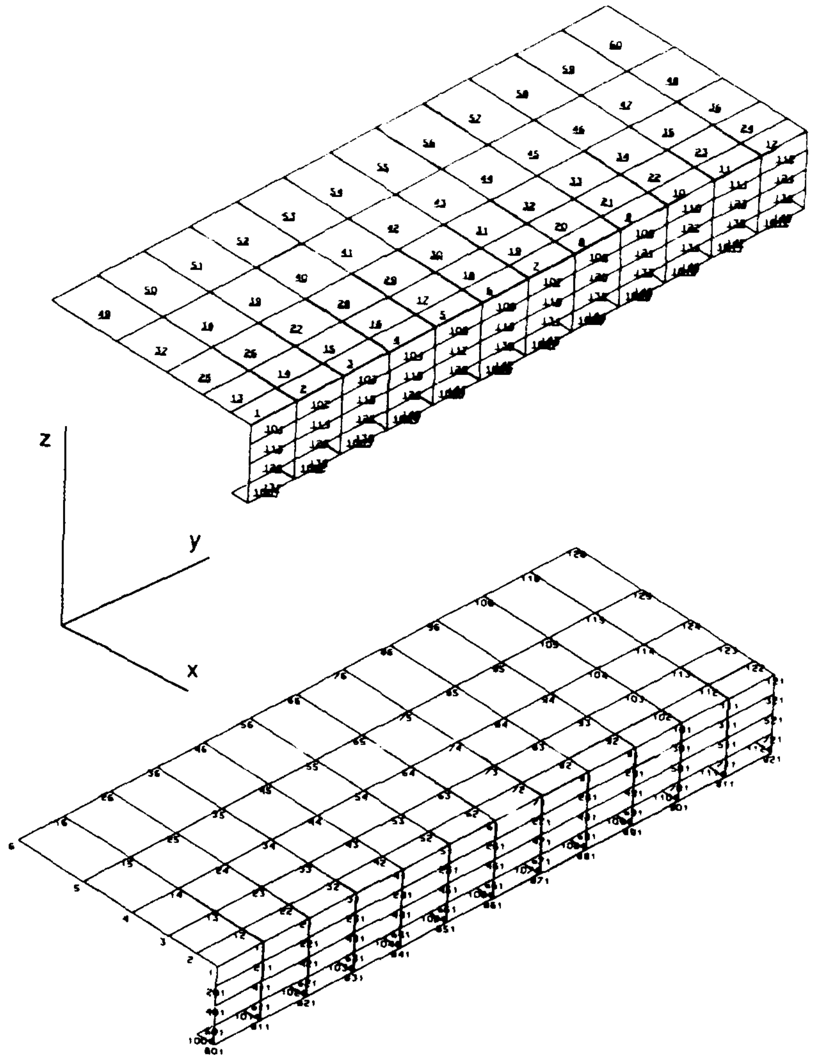

Figure A2 Finite element model of one quarter of the centre panel with the matching element and node numbers

Results

The ABAQUS results (displacements, velocities, accelerations and strains) will be shown in a series of figures. Most of these figures can be compared directly to the figures in [Houlston, 1988]. The results of the comparisons are presented in tables at the end of this section.

Figure A3 shows the displaced shape plots with velocity contours in the z-direction at 4 times, namely 0.5, 4, 10 and 12.5 ms.

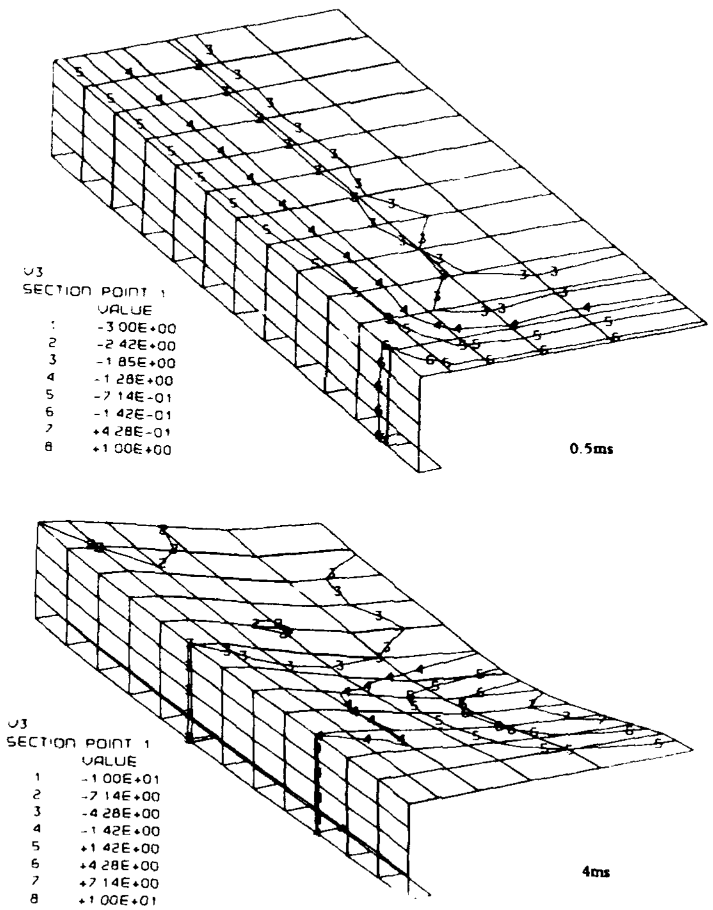

Figure A3 Displaced shape with z-velocity contours (in m/s) at different times, calculated with ABAQUS

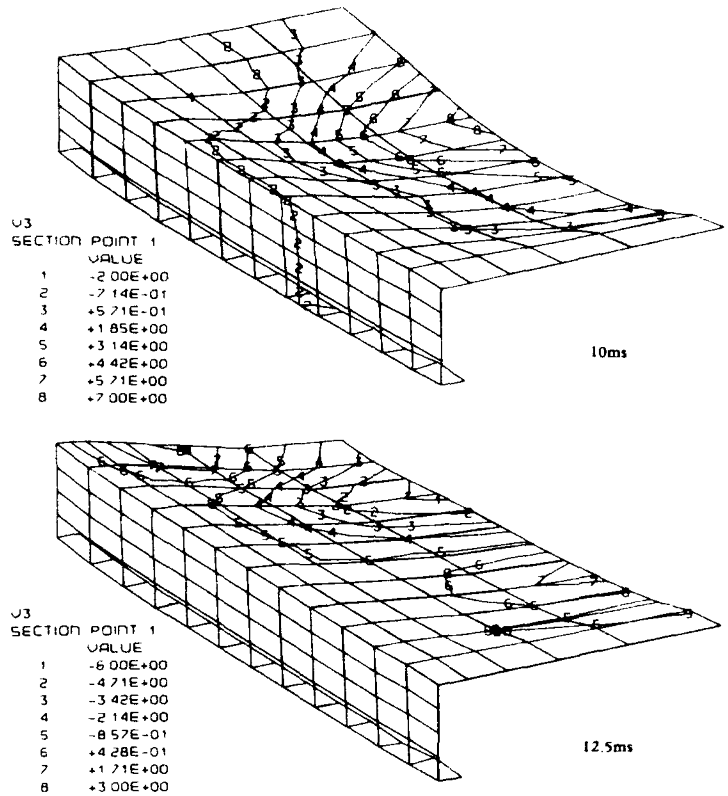

Figure A3 Continued

A number of results are given in [Houlston, 1988] for the centre of the panel and the beam mid-span. These positions coincide with the nodes 6 and 801. The calculated accelerations, displacements and velocities during the first 20 ms for the panel centre (node 6) and the beam mid-span (node 801) are given in Figures A4, A5 and A6. For comparison, the ADINA results given in [Houlston, 1988] are also shown (Figure A7).

The displacements of the panel centre and the beam mid-span for longer times are given in Figures A8 to A11.

Finally, a number of calculated and measured strains are given in [Houlston, 1988] corresponding to the elements 13 and 60. The strains calculated by ABAQUS are given in Figures A12 to A16. The levels of the Von Mises' stresses on the displaced shapes at different times (0.5, 4, 12.5, 20 and 50 ms) are given in Figures A17 to A21. In these figures the displacements are magnified 5 times.

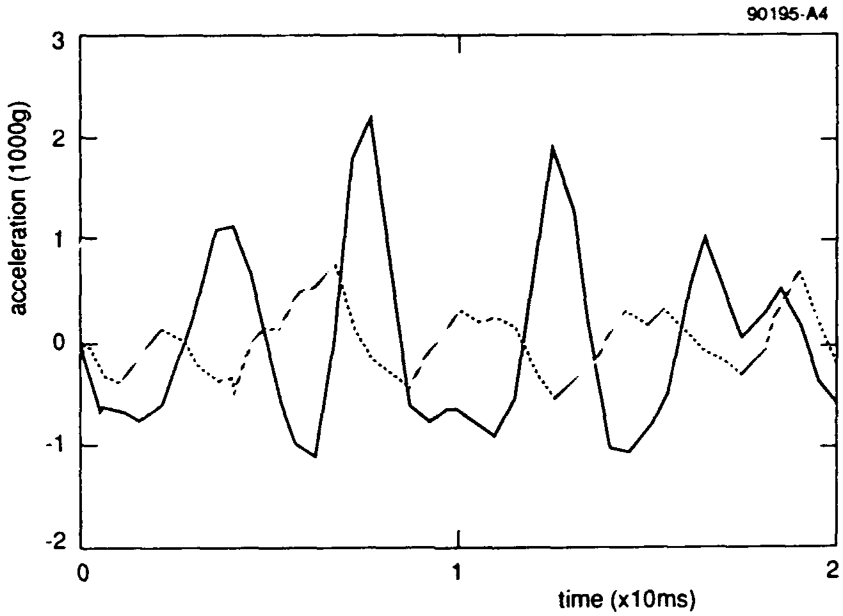

Figure A4 Accelerations in the nodes 6 (line 1, panel centre) and 801 (line 2, beam mid-span), calculated with ABAQUS

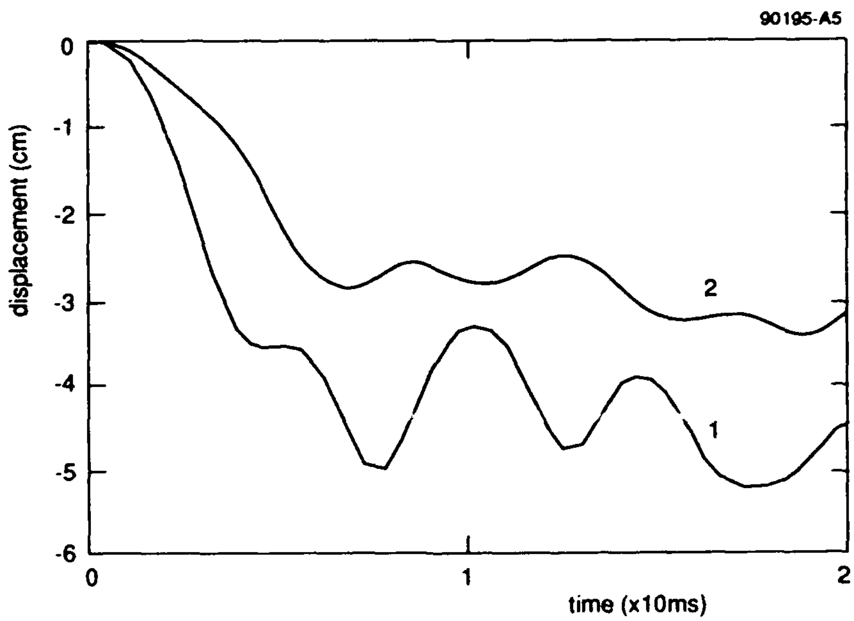

Figure A5 Displacements in the nodes 6 (line 1, panel centre) and 801 (line 2, beam mid-span), calculated with ABAQUS

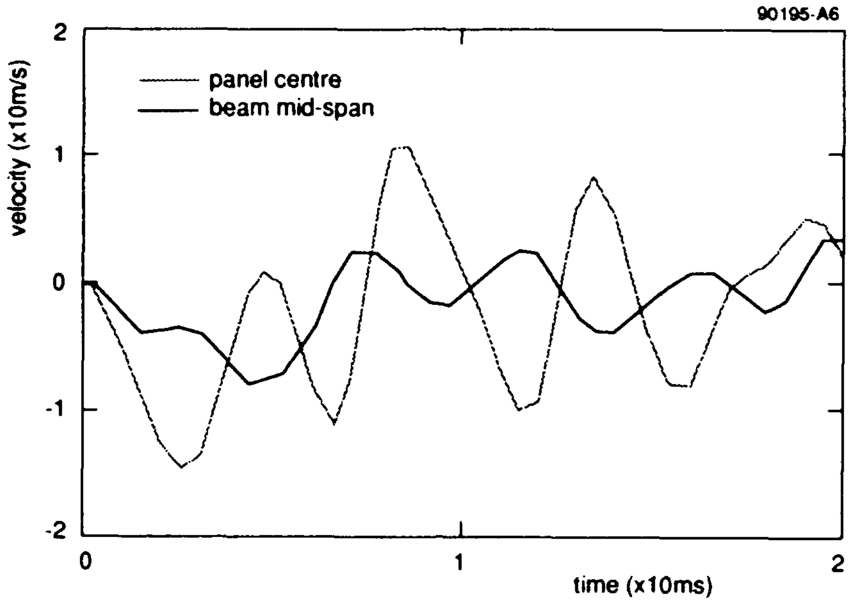

Figure A6 Velocities in the nodes 6 (line 1, panel centre) and 801 (line 2, beam mid-span), calculated with ABAQUS

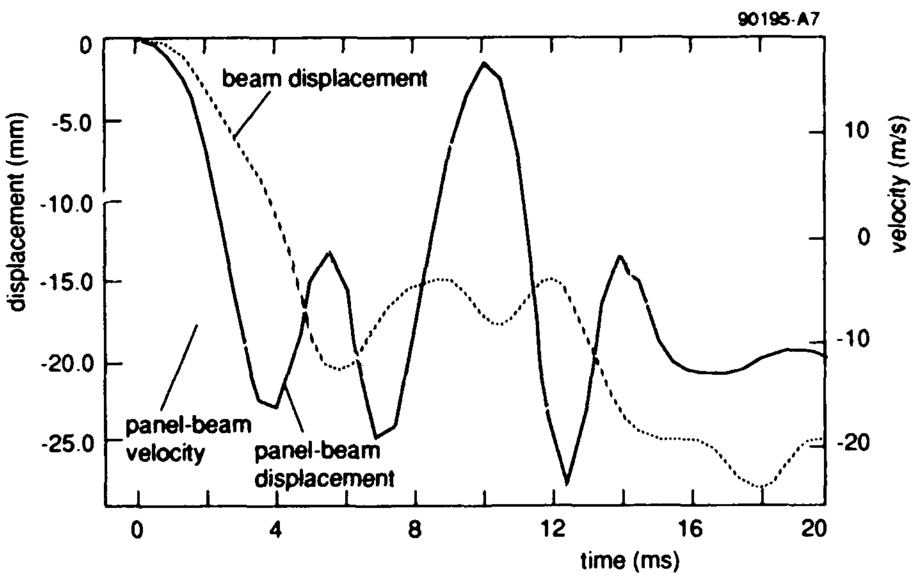

Figure A7 Relative displacements and velocities, calculated with ADINA

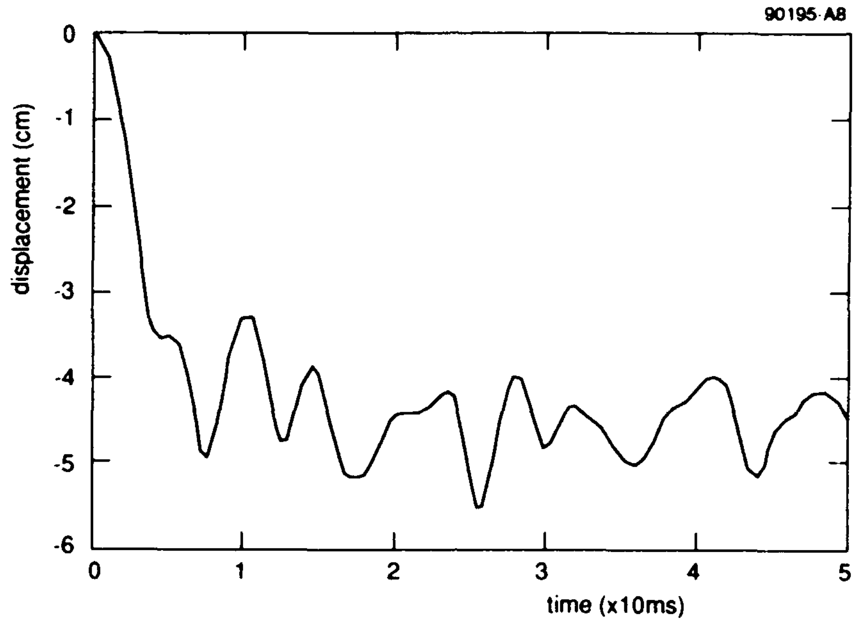

Figure A8 Displacement of node 6 (panel centre) during 50 ms, calculated with ABAQUS

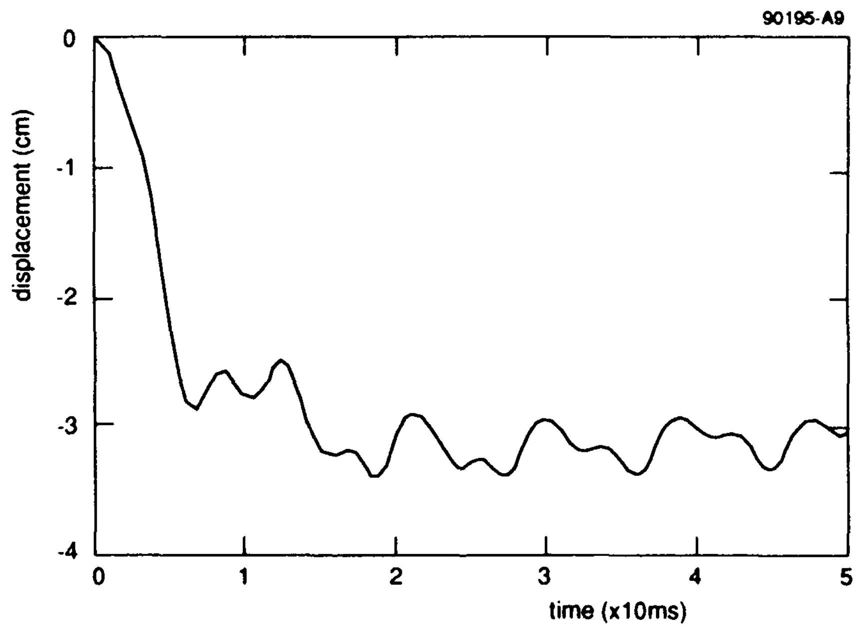

Figure A9 Displacement of node 801 (beam mid-span) during 50 ms, calculated with ABAQUS

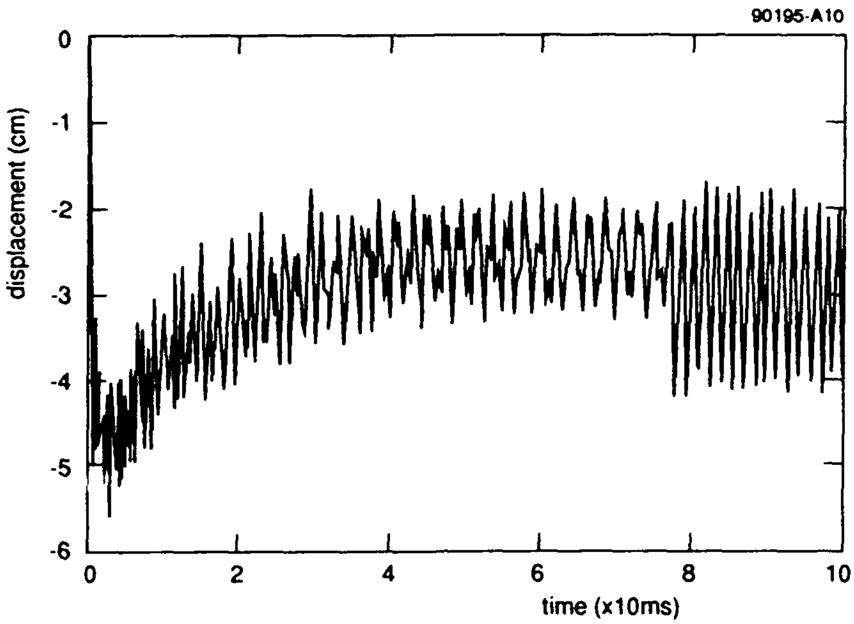

Figure A10 Displacement of node 6 (panel centre) during 1000 ms, calculated with ABAQUS

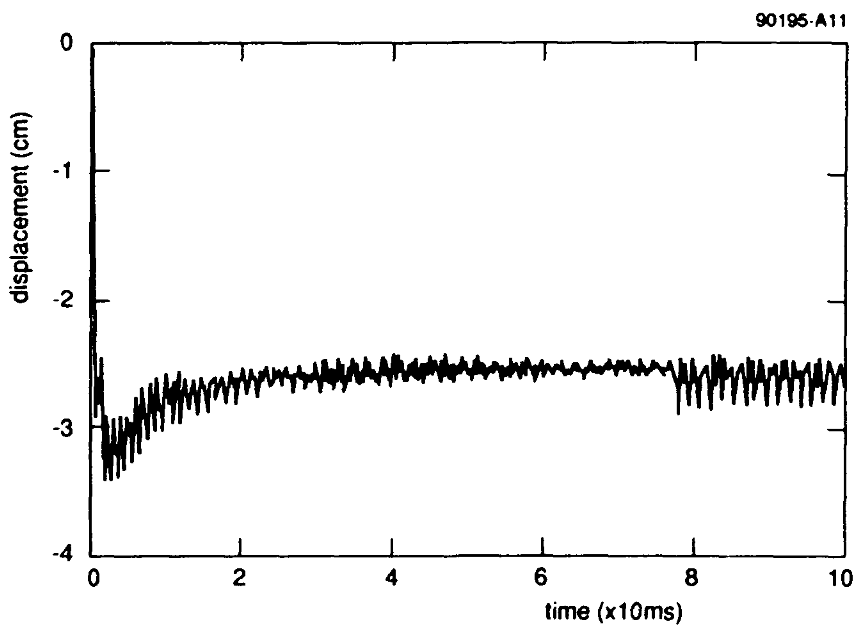

Figure A11 Displacement of node 801 (beam mid-span) during 1000 ms, calculated with ABAQUS

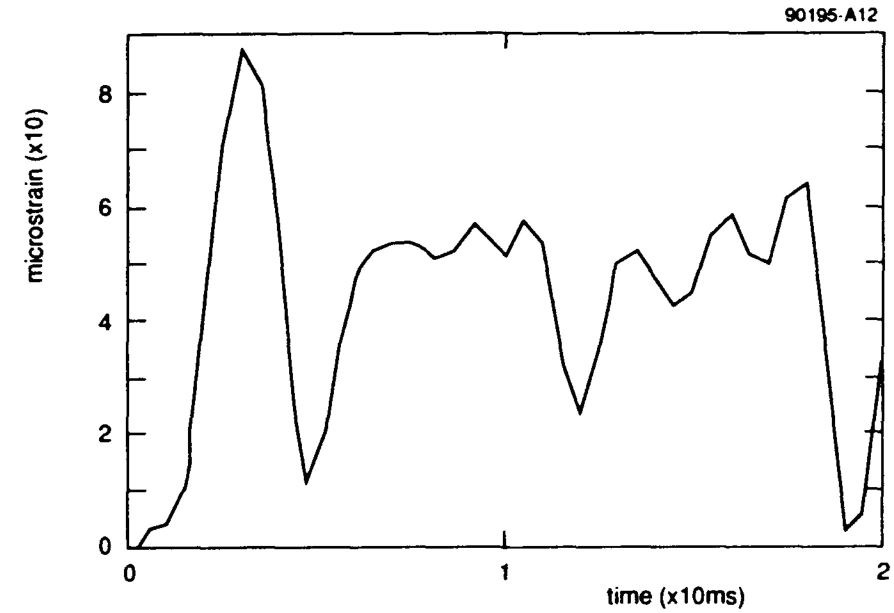

Figure A12 Strain ε_{xx} in the lower layer of element 60, calculated with ABAQUS

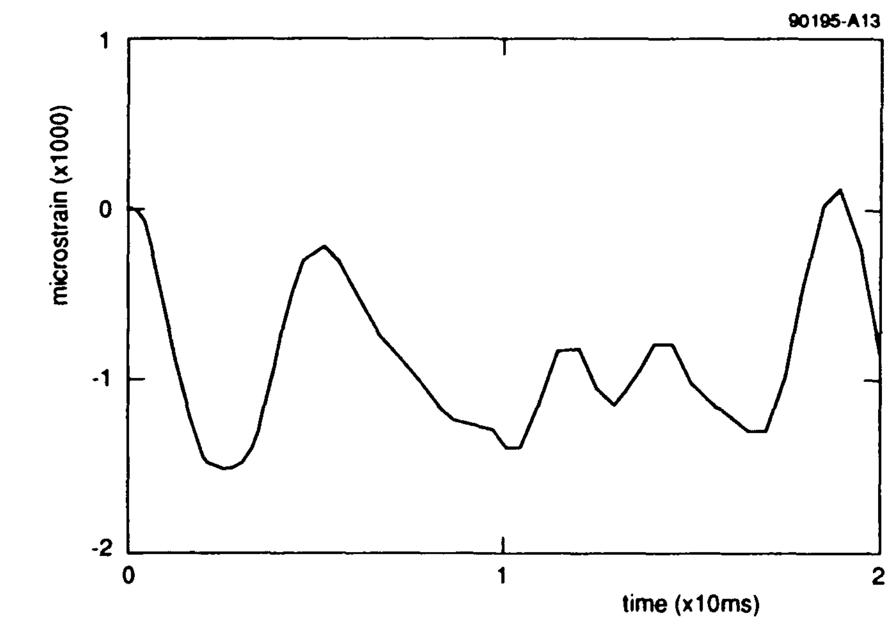

Figure A13 Strain ε_{yy} in the lower layer of element 60, calculated with ABAQUS

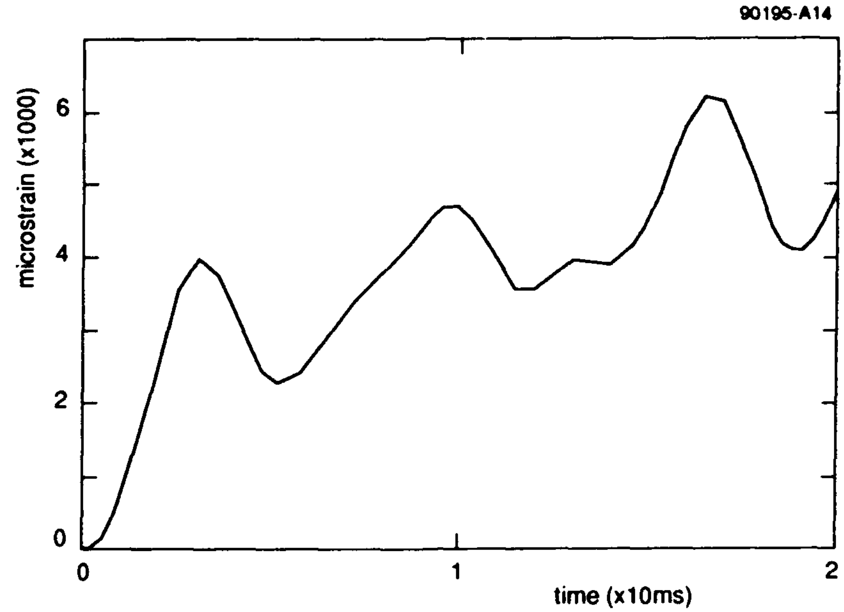

Figure A14 Strain ε_{yy} in the upper layer of element 60, calculated with ABAQUS

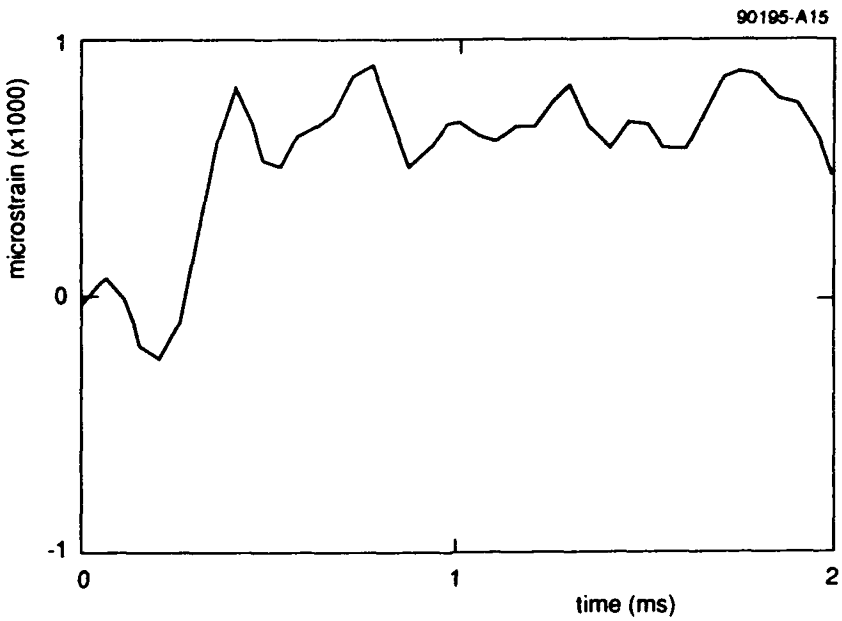

Figure A15 Strain ε_{xx} in the lower layer of element 13, calculated with ABAQUS

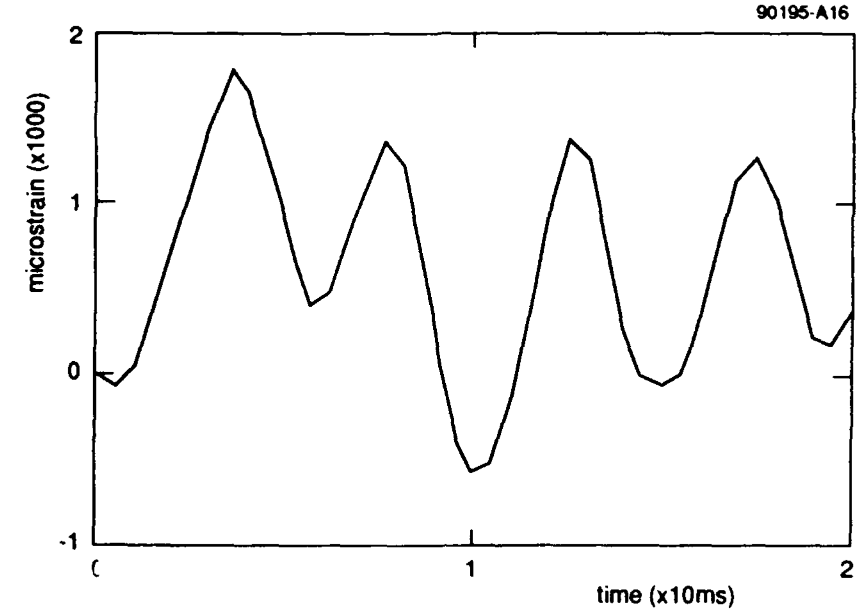

Figure A16 Strain ε_{xx} in the upper layer of element 13, calculated with ABAQUS

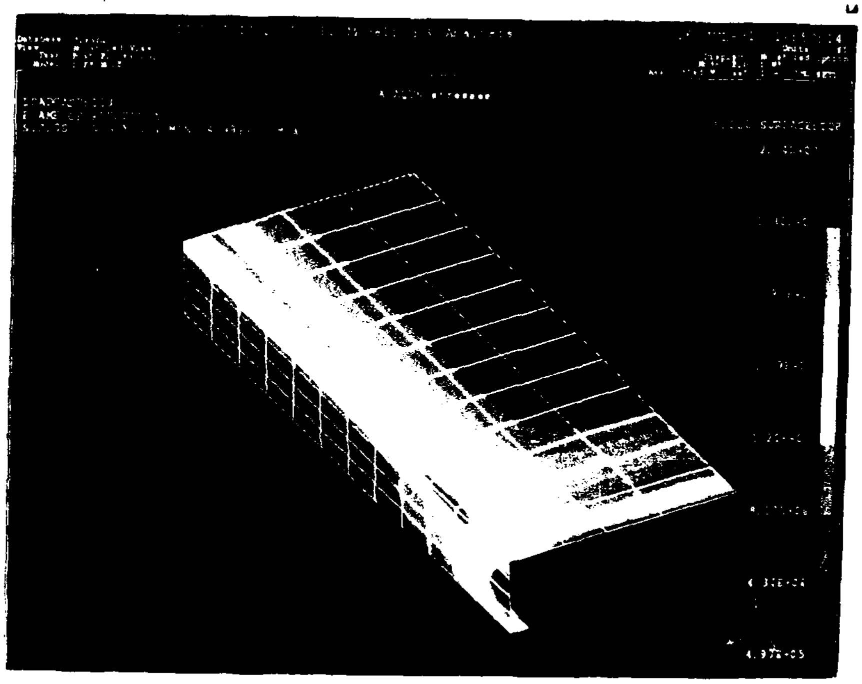

Figure A17 0.5 ms (911127-2)

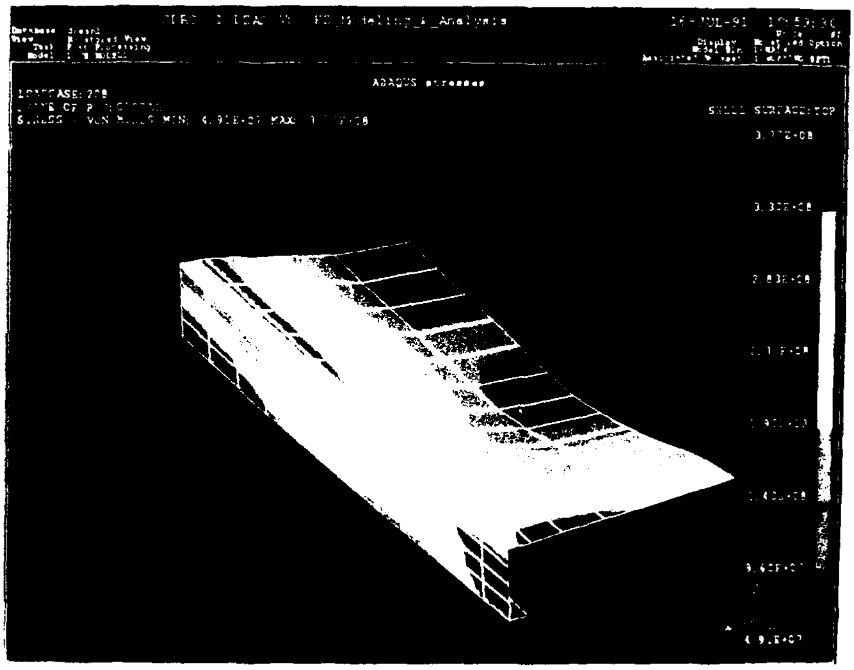

Figure A18 4 ms (911127-5)

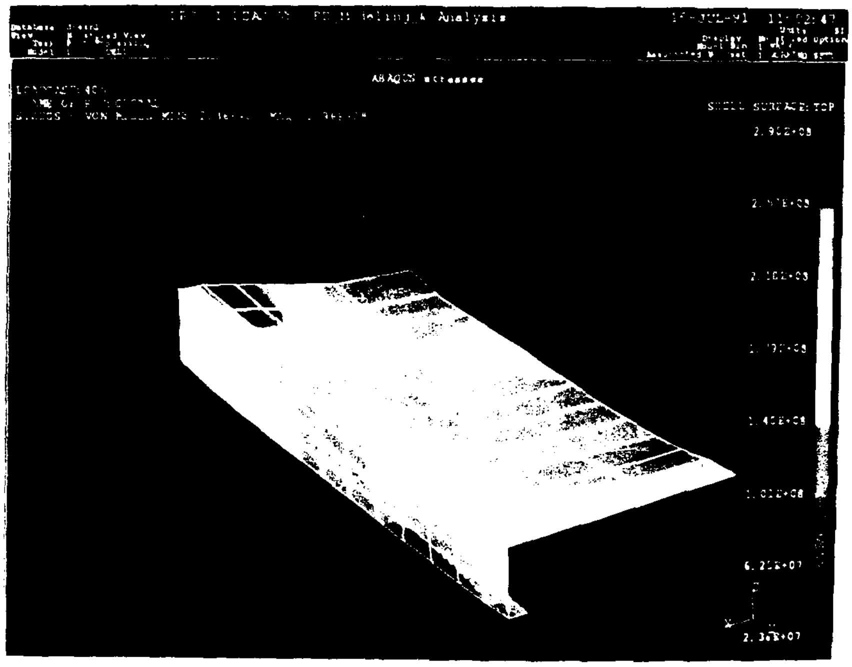

Figure A19 12.5ms (911127-10)

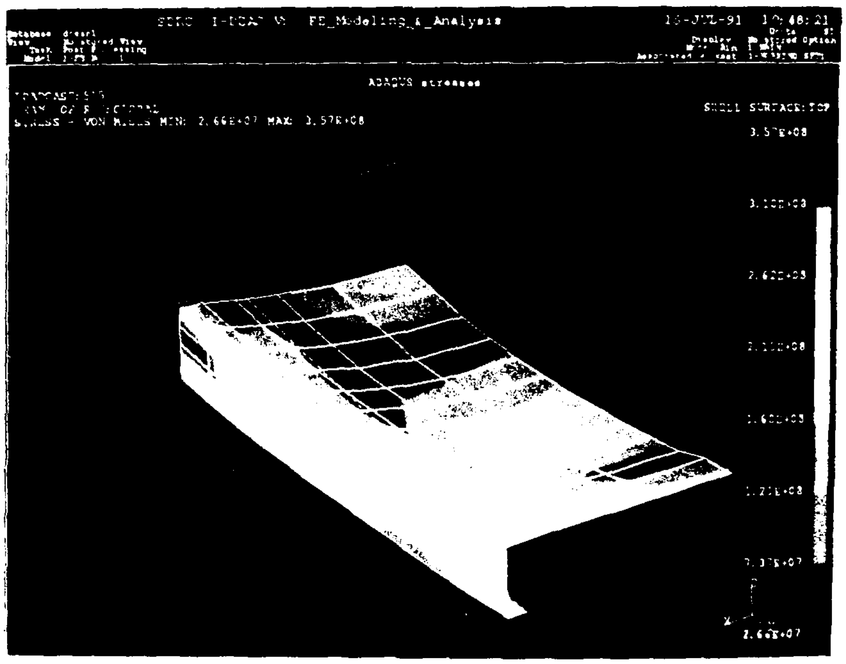

Figure A20 20ms (911127-11)

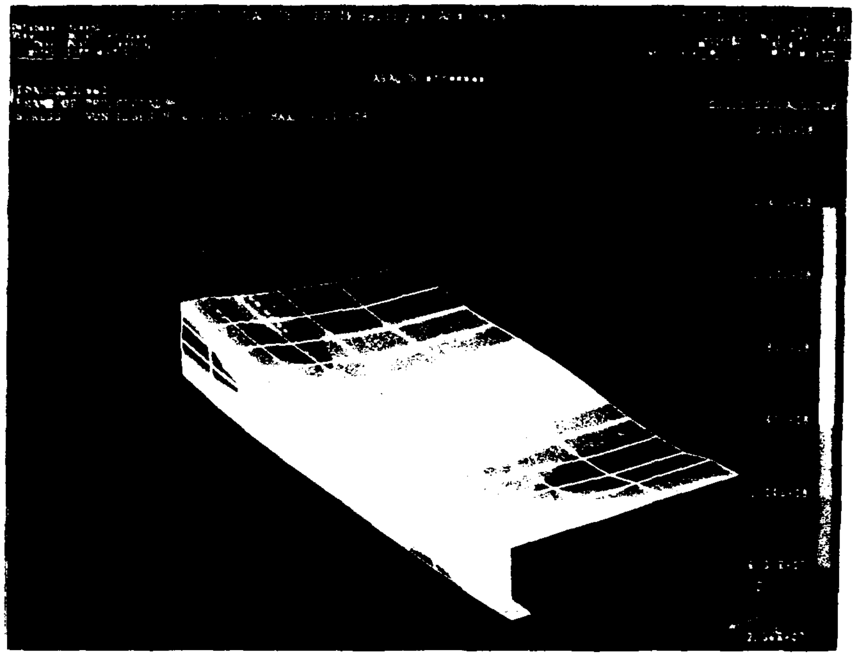

Figure A21 50ms (911127-16)

Comparison of ABAQUS results with experimental and ADINA results

Table A1 Displacements

Position	event. (approx. time) (ms)	ABAQUS (mm)	experiment (mm)	ADINA (mm)
Panel centre	first minimum (8)	-50	-44	-42
	first maximum (10)	-33	-35	-18
	final (700)	-35	-18	-20 (average)
Beam mid-span	first minimum (7)	-29	-23	-20
	first maximum (12)	-25	-17	-11
	final (700)	-25	-14	-19 (average)

Table A2 Accelerations

Position	event, (approx. time) (ms)	ABAQUS (g)	experiment (g)	ADINA (g)
Panel centre	first mimimum (1.8)	-783	-885	-884
	first maximum (3.3)	1145	1067	1356
Beam mid-span	first mimimum (0.5)	-422	-208	-324
	first maximum (4.0)	120	50	148

Table A3 Strain

Position	event, (approx. time) (ms)	ABAQUS (µstrain)	experiment (µstrain)	ADINA (µstrain)
ε_{xx}, element 60	first maximum (3)	87	292	368
(lower layer)	first mimimum (6.5)	13	-97	43
ε_{yy}, element 60	first maximum (7)	-216	-	-66
(lower layer)	first mimimum (1.5)	-1518	-	-1556
ε_{yy}, element 60	first maximum (3)	3964	-	2278
(upper layer)	first mimimum (6)	2277	-	1215
ε_{xx}, element 13	first maximum (6.5)	915	1070	1318
(lower layer)	first mimimum (2)	-240	-1482	-494
ε_{xx}, element 13	first maximum (4)	1770	3585	5800
(upper layer)	first mimimum (10)	-580	2050	2560

ANNEX 2 INPUT DATA AND RESULTS OF ROOFDIER SIMULATION

Input data

The length over height ratio of the bulkhead is large, so it will act like a beam clamped between the two decks and only a quarter of the part between two stiffeners, and half the stiffener needs to be modelled. The dimensions of this part are:

width	:	0.2665 m
height	:	1.19 m
thickness	:	6.34 mm

Stiffener (these dimensions are half the T stiffener):

web height	:	101.6 mm
web thickness	:	1.95 mm
flange thickness	:	3.9 mm
flange width	:	28.6 mm

The plate was modelled with 10x20 shell elements (ABAQUS element type S4R, with 5 section points). The stiffener was modelled with 8x18 + 5 shell elements (ABAQUS element type S4R, with 3 section points), instead of 8x20 elements because the stiffener is not welded to the deck. Figure B1 presents a plot of the mesh with the matching element and node numbers.

The boundary conditions that were used are:

- fully fixed along the bottom edge (elements 101 to 110);
- symmetry along the two vertical edges;
- symmetry along the top edge.

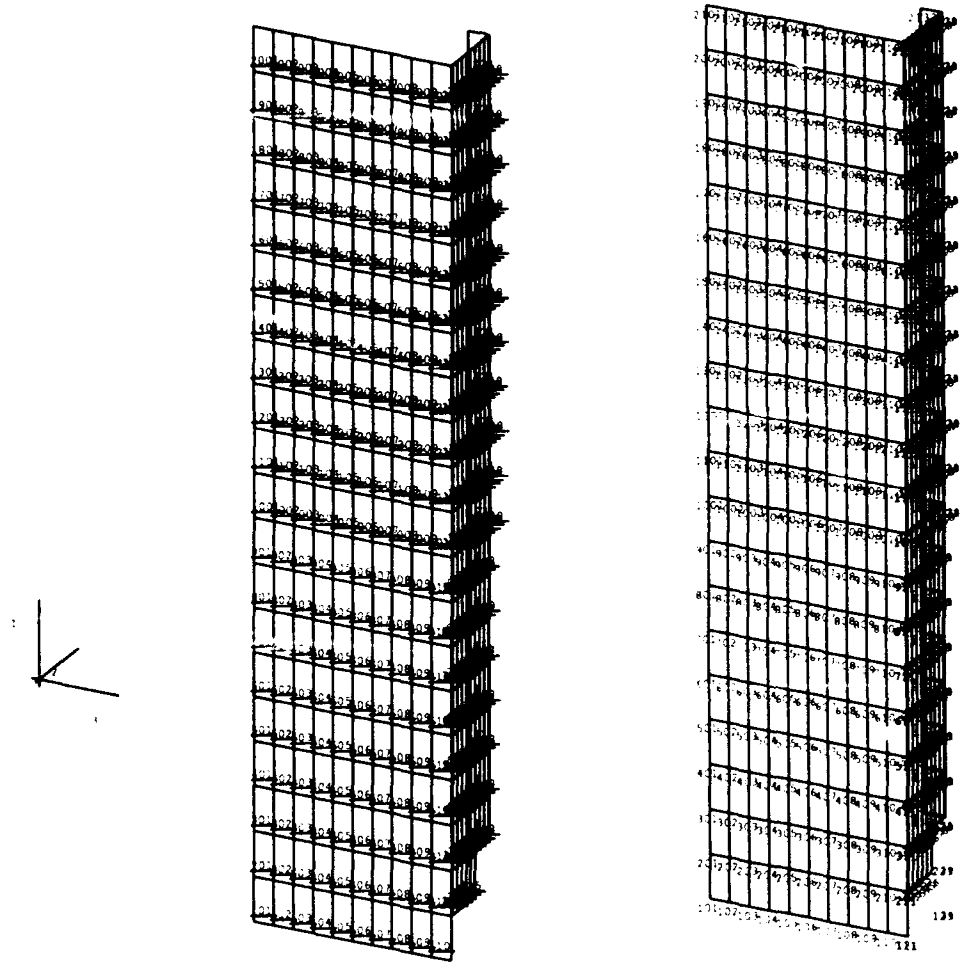

Figure B1 Mesh of a part of the bulkhead. Figure a gives the element numbers and figure b gives the node numbers

The steel of the plate and the stiffeners were modelled as an ideal elastic-plastic material using Von Mises' yield criterion. The yield strength was taken as 275 MPa, in accordance with tests performed on the steel of the ships [v/d Brand and Muller, 1987]. Strain-rate sensitivity of the yield stress was included in the material model. For this, the Cowper-Symonds model was used:

ε_{pl} $= D\ (\sigma/\sigma_0 - 1)^p$, for $\sigma > \sigma_0$,

where ε_{pl} = uniaxial equivalent plastic strain rate,

σ = effective yield stress at a non-zero strain rate,

σ_0 = static yield stress, and

D and p are material parameters

To summarize, the used material properties were:

Young's modulus	: 210 GPa
Poisson's ratio	: 0.3
Density	: 7800 kg/m^3
Yield strength	: 275 MPa
D	= 40.4 1/s and p = 5.

The calculation was made with a transient dynamic analysis. Non-linear geometric effects were included. The Hilber-Hughes a-method was used for the implicit time integration, with the numerical damping ratio a set to -0.05 [ABAQUS Users' Manual, 1989]. Accurate calculations were made up to a time of 27 ms. Automatic time-step choice was used, with an initial time-step size of 0.05 ms, a maximum time-step size of 0.1 ms, tolerance PTOL = 2500, tolerance MTOL = 125, and tolerance HAFTOL = 2.5.10^5. Initial calculations showed that no plastic deformation took place after 27 ms. After 27 ms, the calculation was continued with a larger time-step, and more damping. This was done to obtain the permanent deformed shape in an efficient way. The computed values in the period between 27 ms and 3000 ms are therefore not accurate, in the sense that the vibrations are quickly dampened away and only the response to the quasi-static load is computed.

Results

The calculated vertical displacements during the first 35 ms of the beam mid-span (node 2111) and panel centre (node 2101) nodes are given for a the dynamic calculation using a non-linear material and including geometric non-linearities and with strain-rate dependent yield stress (Figure B2).
The calculated kinetic energy (line 1), elastic strain energy (line 2) and energy dissipated in plastic deformation (line 3) summed on the entire model is given in Figure B3.
Figures B4-B13 show the measured and calculated strain histories on a 300 ms and on a 3 s time base. These results are summarized in Table 4.

Figures B14 and B15 give the levels of Von Mises' strain at 27 and 3000 ms. Figure B15 can be compared to Figure 12, which gives the static strain distribution under a load of 188 kPa. The peak displacements are comparable in these two cases. In the figures the displacements are magnified 5 times. It must be realised that no load is present in Figure B15, the deformation is due to residual stresses. In Figure 12, the panel is still loaded by a pressure of 188 kPa. Both figures show that the strain is concentrated near the clamped edge and in the middle of the stiffener. The rest of the plate is below the static yield strain. This result raised the question whether the strain concentration could be the result of localization.

Localization would concentrate all the strain in one row of elements, even if the mesh were refined. This causes a number of problems. In the first place, the calculated strains in and near those elements become unreliable. In the second place, if the element is deformed in tension, the dissipated energy becomes less if the element size is reduced. This affects the results in the complete model. With bending deformation, this does not occur.

Indeed, a calculation with a refined mesh showed that the strain concentration was caused by numerical localization. Because the deformation is bending deformation, this only affects the calculated strains near the clamped edge of the bulkhead.

Figures B16 through B22 present the Von Mises' stress at the outside surface of the plate at consecutive points in time. Figures B16 to B18, at 1.25, 2.25 and 6.0 ms, show a bending wave running from the supported end of the plate to the middle. It is clear that the deformed geometry at these points of time does not conform to the deformed geometry under a static load. Figure B21, at 27 ms, shows membrane stresses. Figure B22 shows the residual stresses after the removal of the load at 3000 ms. Figure B23 shows the Von Mises' stress at the inside surface of the plate at 27 ms. It can be compared with Figure B21, which indicates that the stress in the middle is composed of membrane stress superimposed on bending stress.

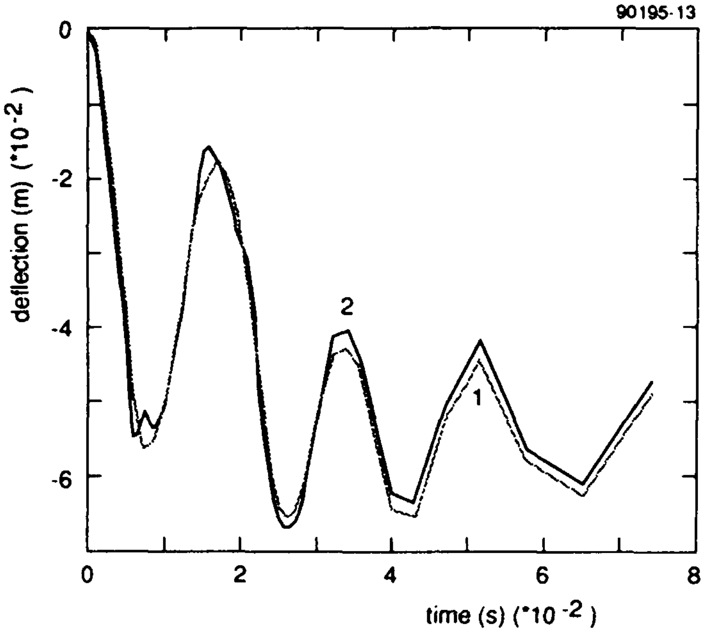

Figure B2 Displacement of beam mid-span (node 2111, line 2) and panel centre (node 2101, line 1), obtained with a dynamic ABAQUS calculation, using a non-linear material and including geometric non-linearities and including strain-rate dependency of the yield stress

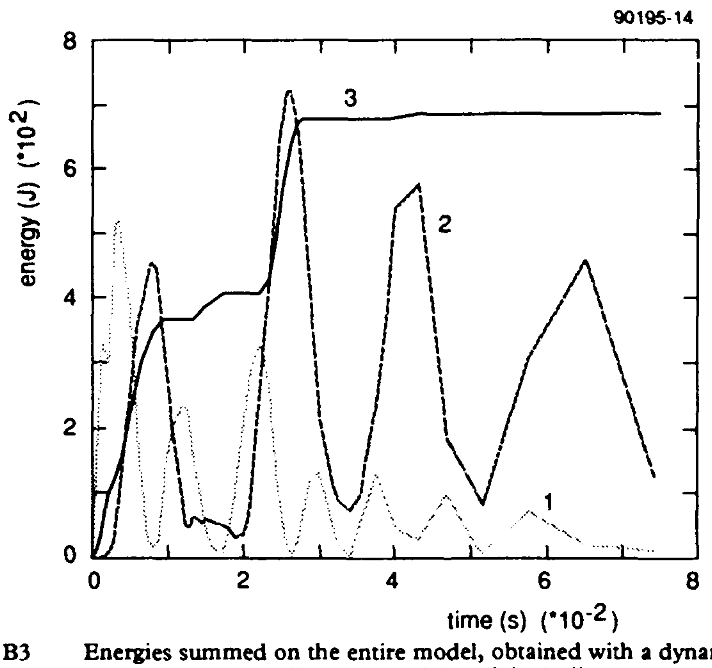

Figure B3 Energies summed on the entire model, obtained with a dynamic ABAQUS calculation, using a non-linear material and including geometric non-linearities and including strain-rate dependency of the yield stress (line 1 gives kinetic energy, line 2 gives elastic strain energy, line 3 gives energy dissipated in plastic deformation)

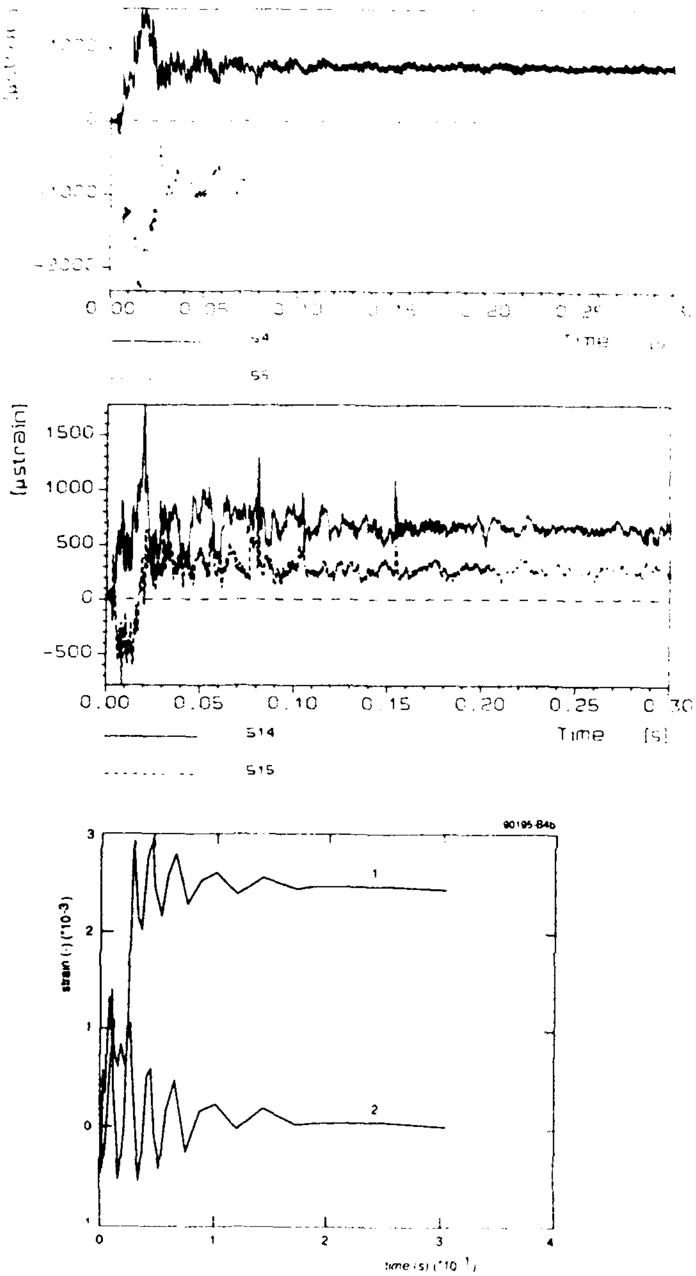

Figure B4 Strain histories during 300 ms at 80 mm from stiffener along model bottom edge
S4, S14 measured inside experiment compartment
line 2 calculated for inside position
S5, S15 measured outside experiment compartment
line 1 calcula•ed for outside position

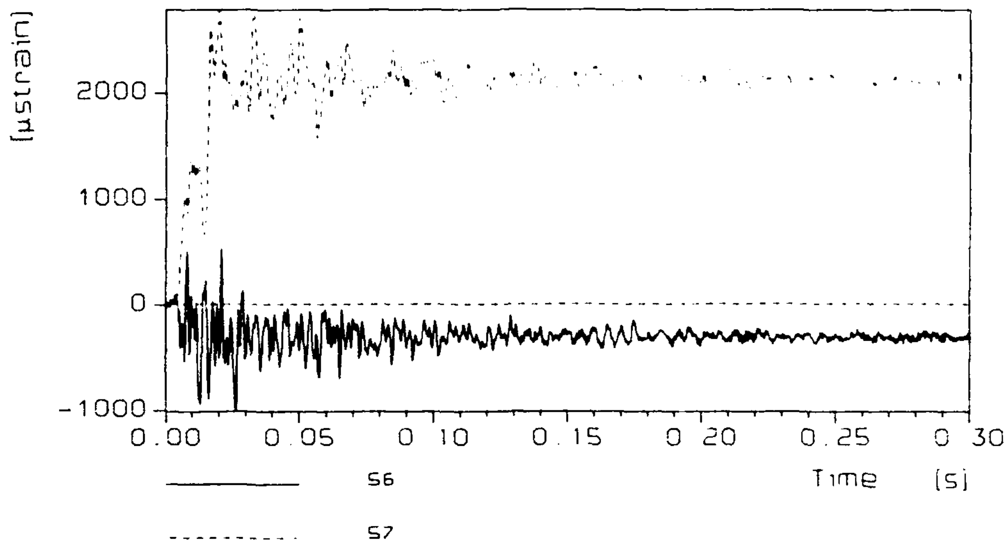

90195-B5b

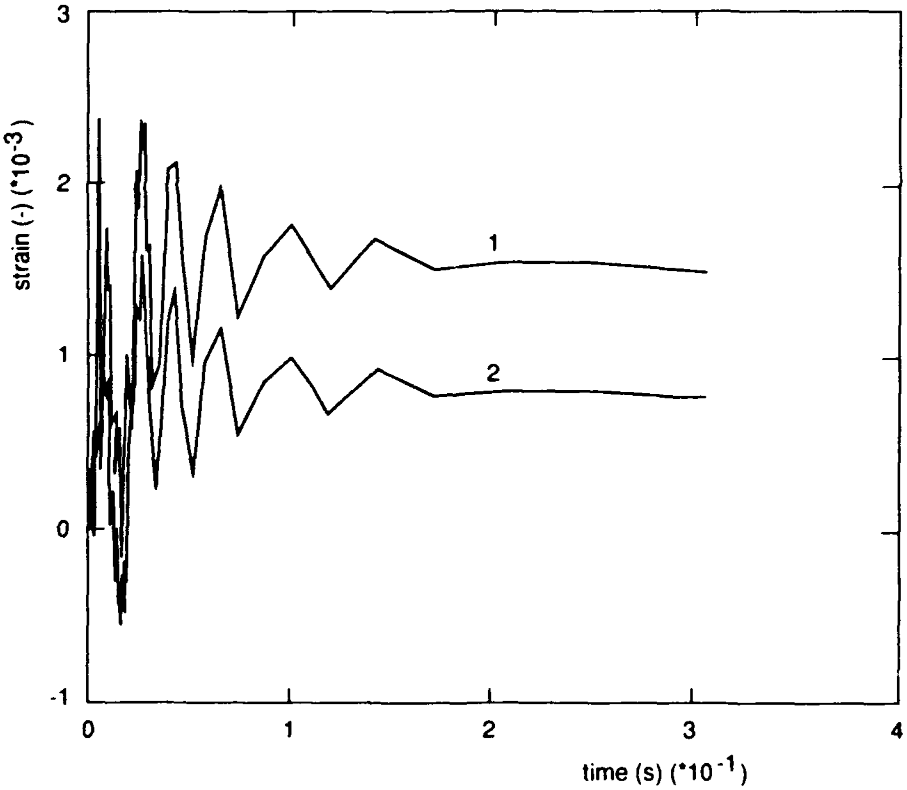

Figure B5 Strain histories during 300 ms at 260 mm from stiffener along model top edge
S6 measured inside experiment compartment
line 2 calculated for inside position
S7 measured outside experiment compartment
line 1 calculated for outside position

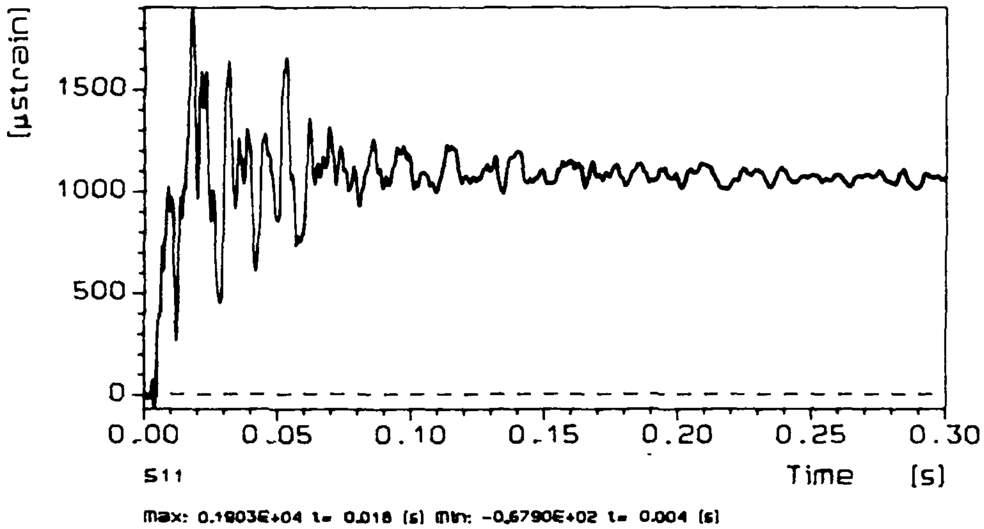

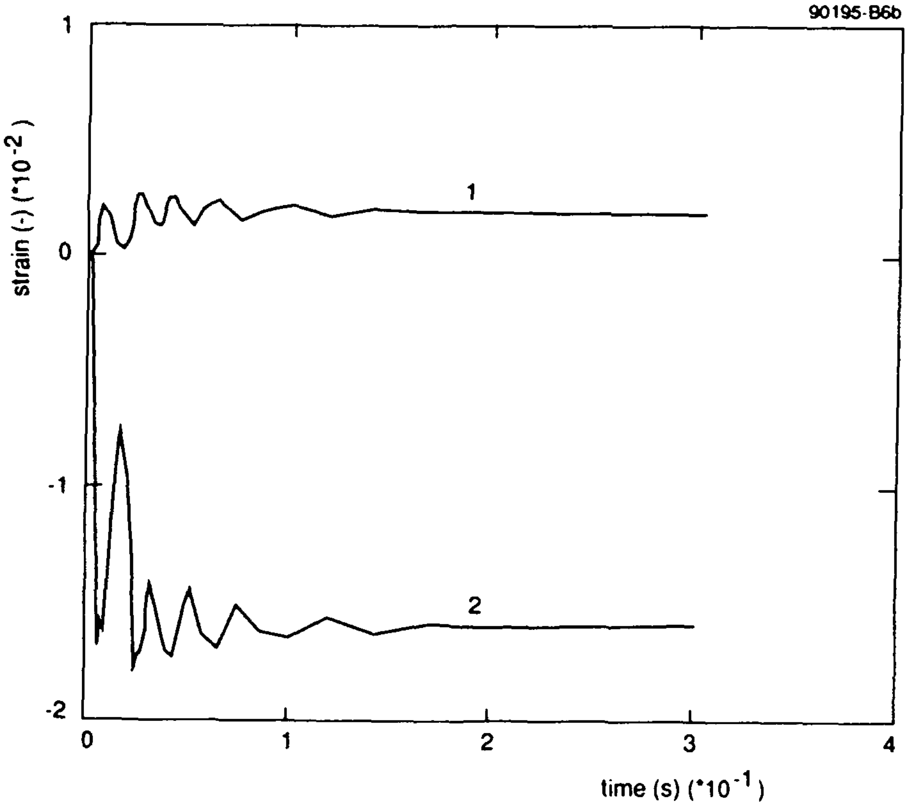

Figure B6 Strain histories during 300 ms at centre of stiffener along model top edge
line 2 calculated for inside position
S11 measured outside experiment compartment
line 1 calculated for outside position

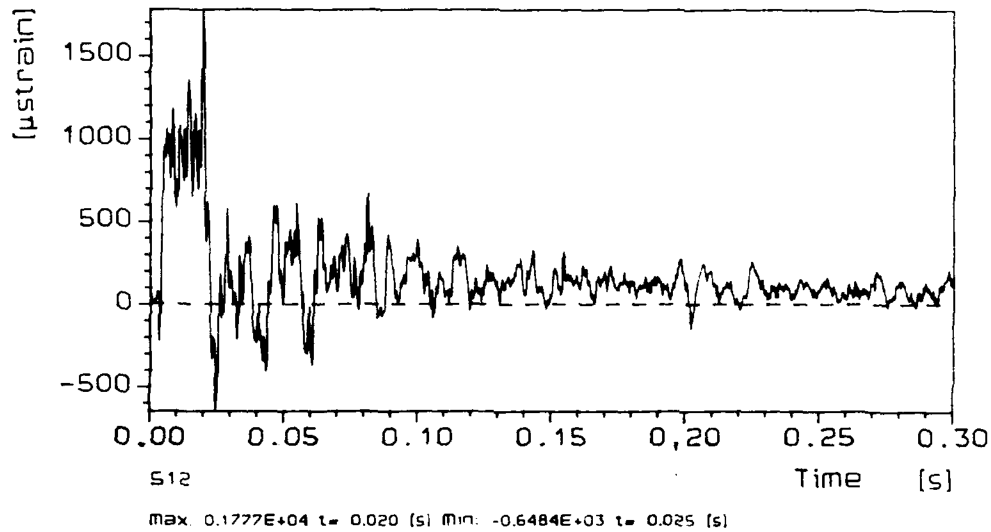

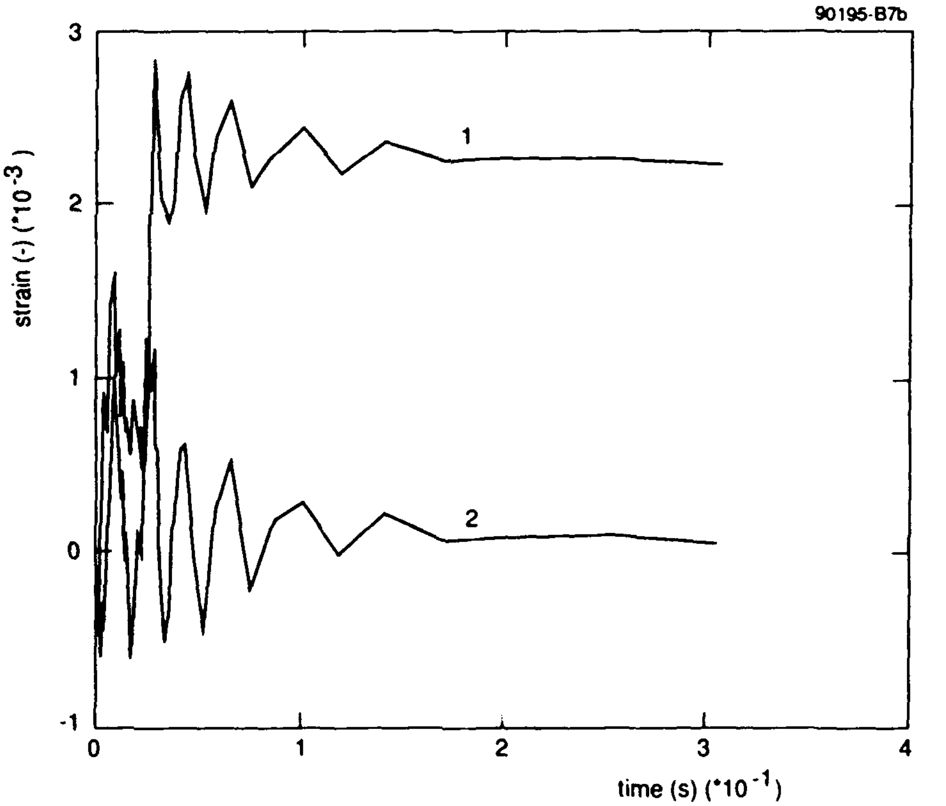

Figure B7 Strain histories during 300 ms at 260 mm from stiffener along model bottom edge
S12 measured inside experiment compartment
line 2 calculated for inside positionline
1 calculated for outside position

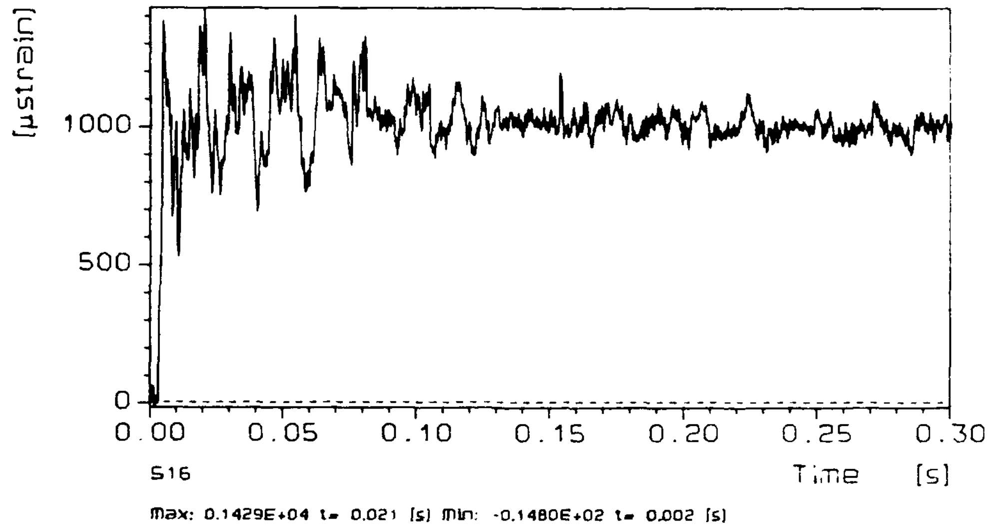

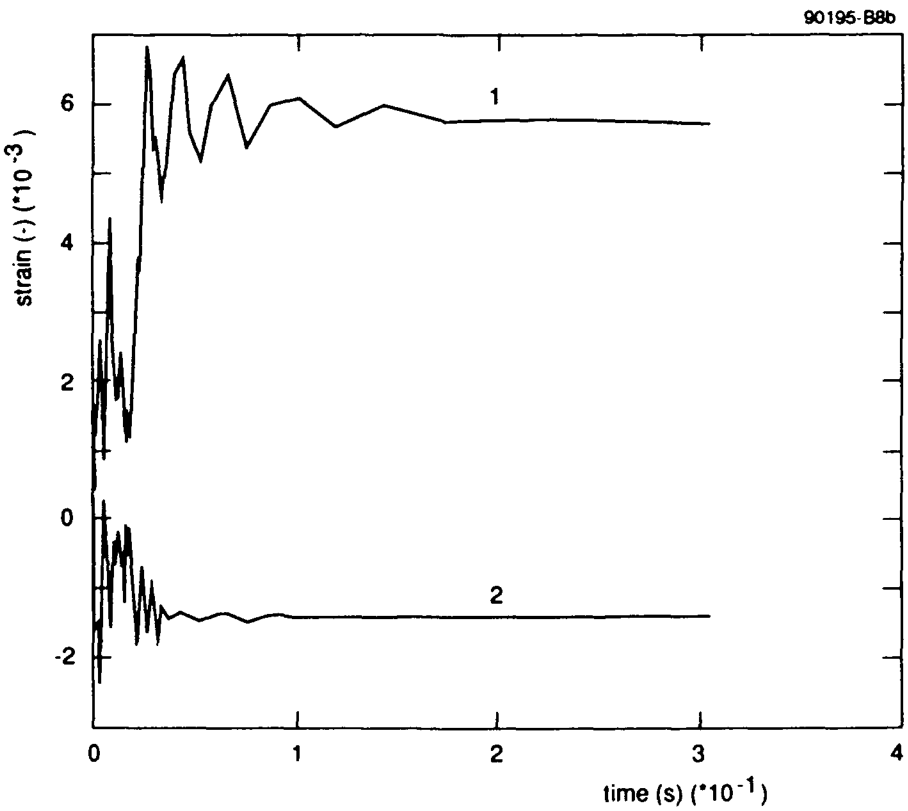

Figure B8 Strain histories during 300 ms at back of stiffener along model bottom edge
line 2 calculated for inside position
S16 measured outside experiment compartment
line 1 calculated for outside position

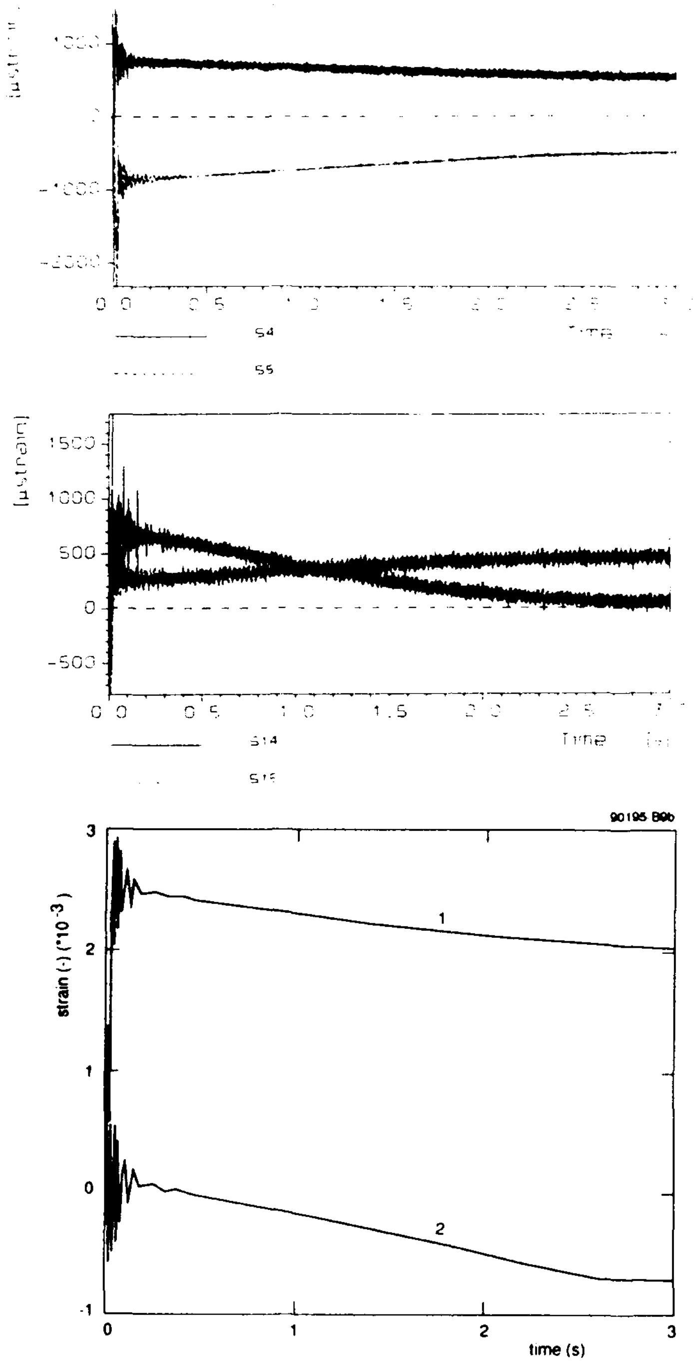

Figure B9 Strain histories during 3 s at 80 mm from stiffener along model bottom edge
S4, S14 measured inside experiment compartment
line 2 calculated for inside position
S5, S15 measured outside experiment compartment
line 1 calculated for outside position

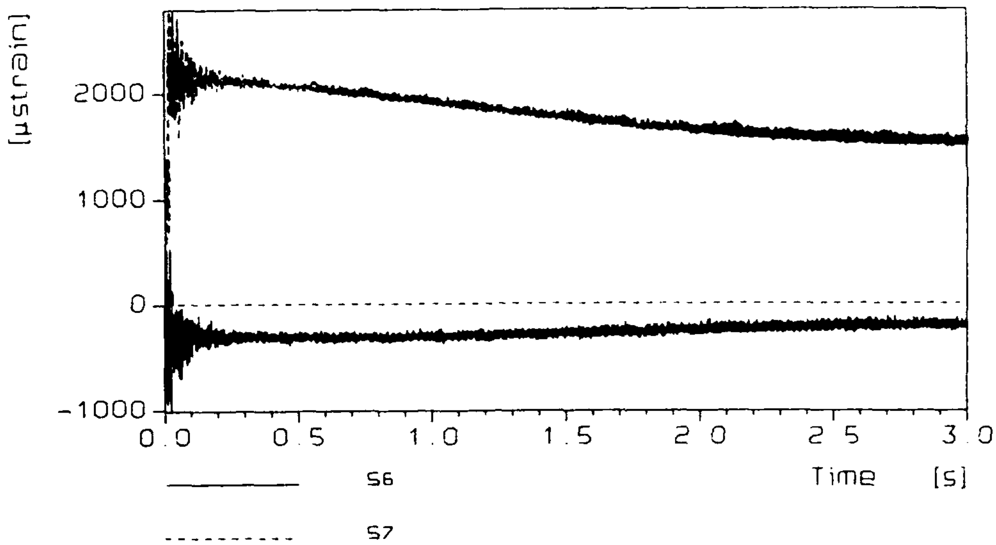

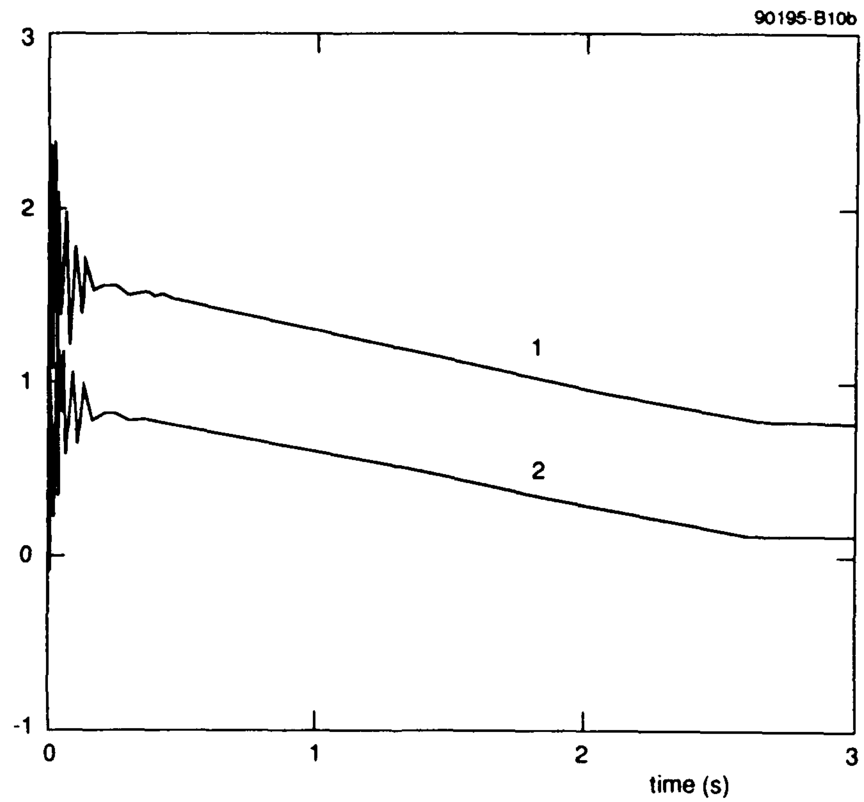

Figure B10 Strain histories during 3 s at 260 mm from stiffener along model top edge S6 measured inside experiment compartment iine 2 calculated for inside position S7 measured outside experiment compartment line 1 calculated for outside position

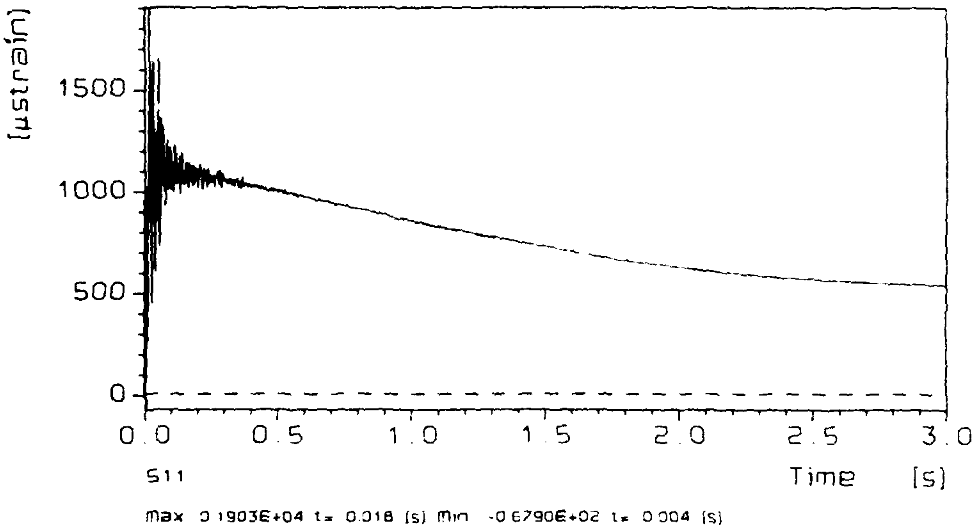

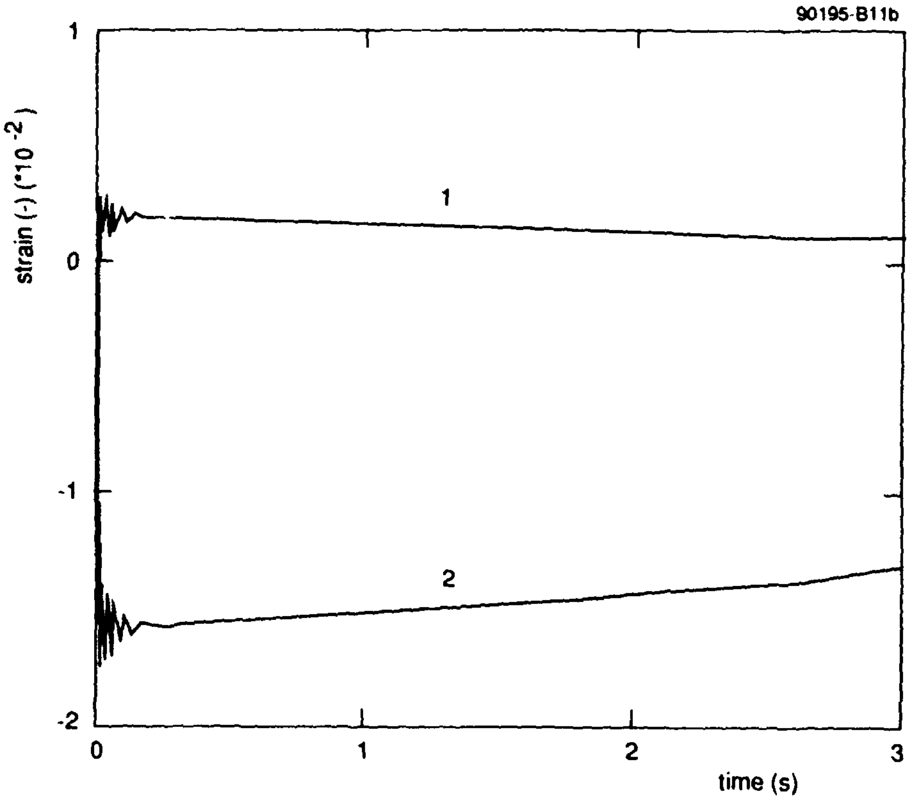

Figure B11 Strain histories during 3 s at centre of stiffener along model top edge
line 2 calculated for inside position
S11 measured outside experiment compartment
line 1 calculated for outside position

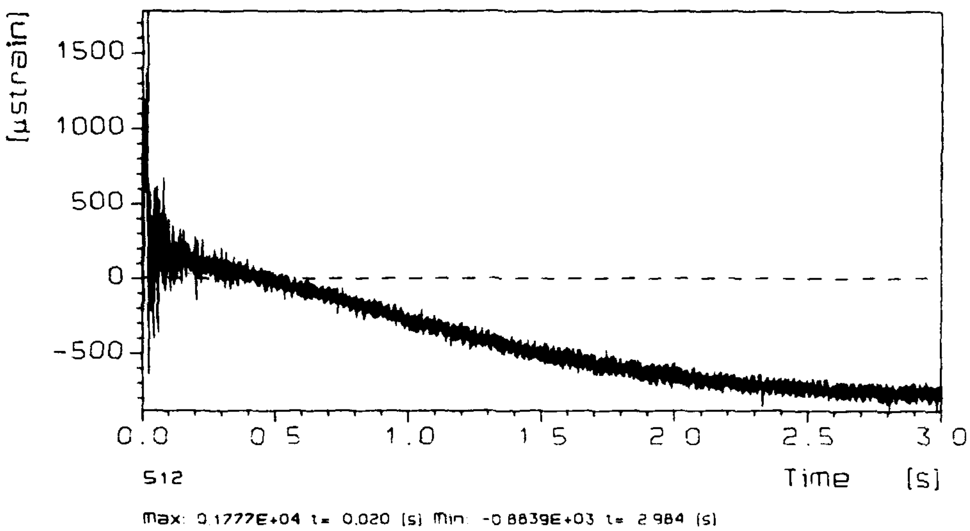

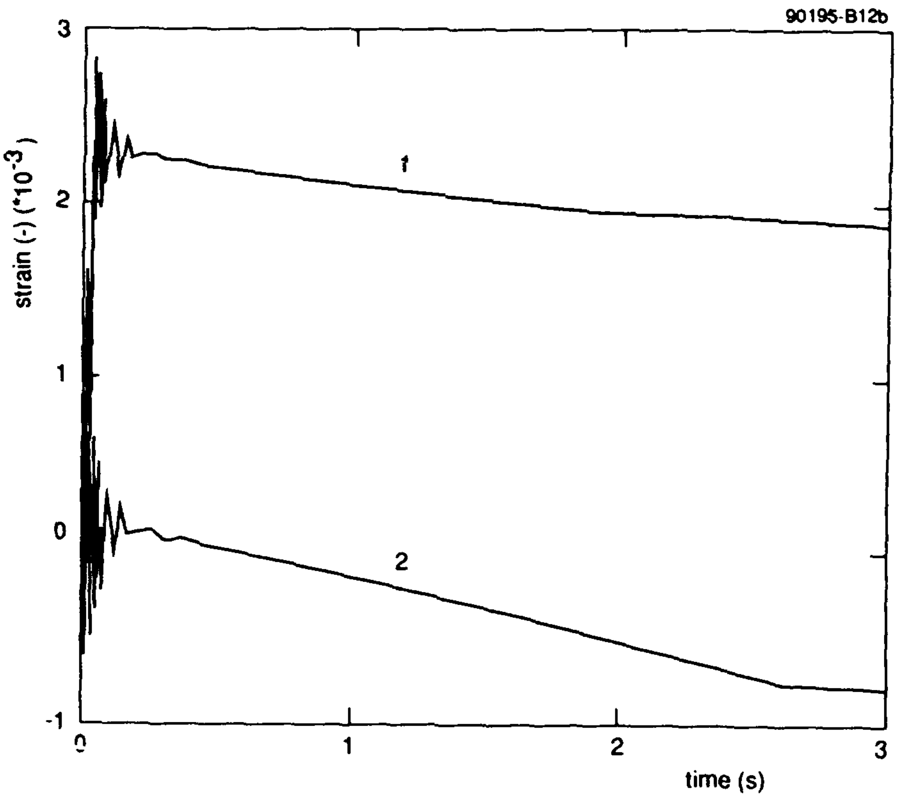

Figure B12 Strain histories during 3 s at 260 mm from stiffener along model bottom edge
S12 measured inside experiment compartment
line 2 calculated for inside position line
1 calculated for outside position

PML 292490195

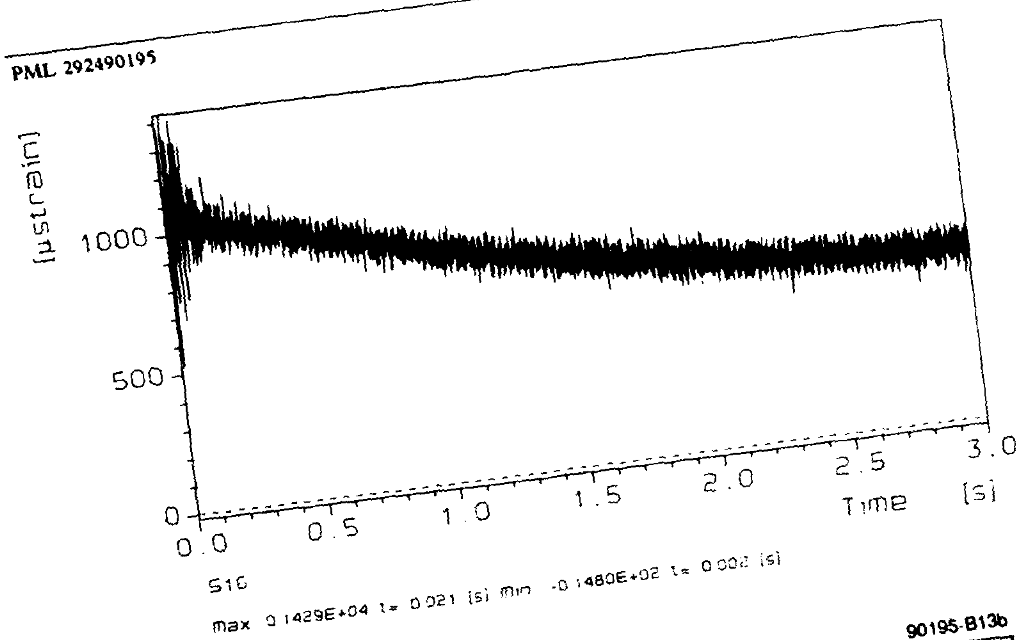

90195-B13b

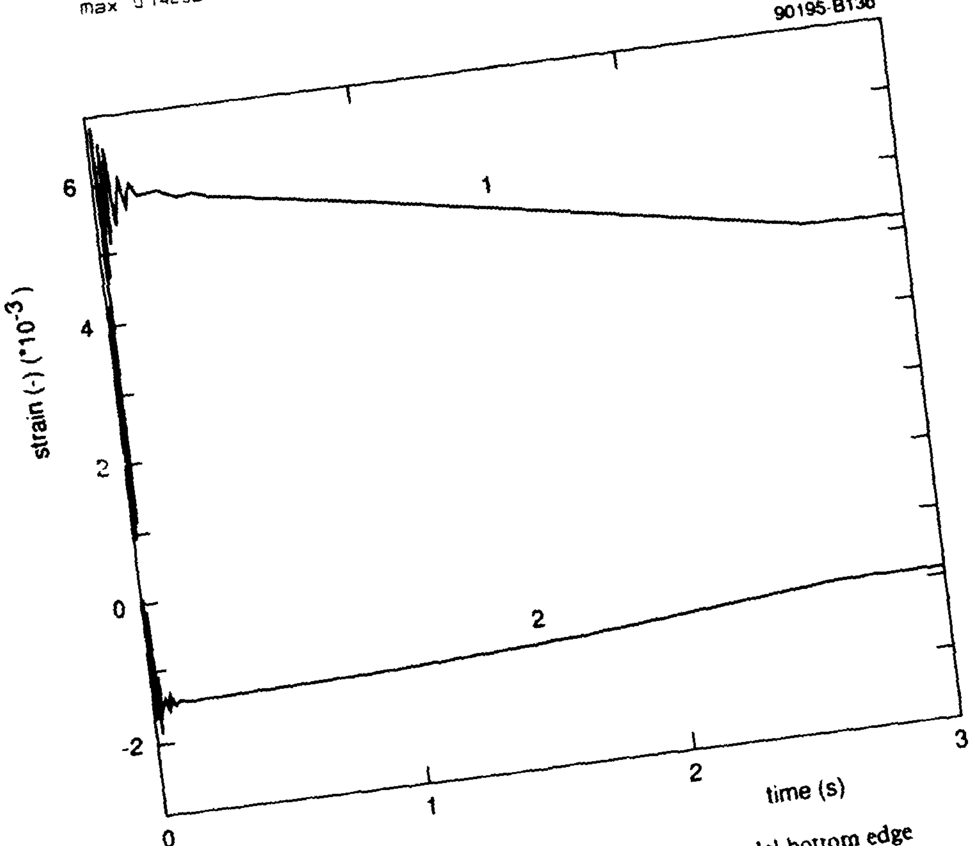

Figure B13 Strain histories during 3 s at back of stiffener along model bottom edge
line 2 calculated for inside position
S16 measured outside experiment compartment
line 1 calculated for outside position

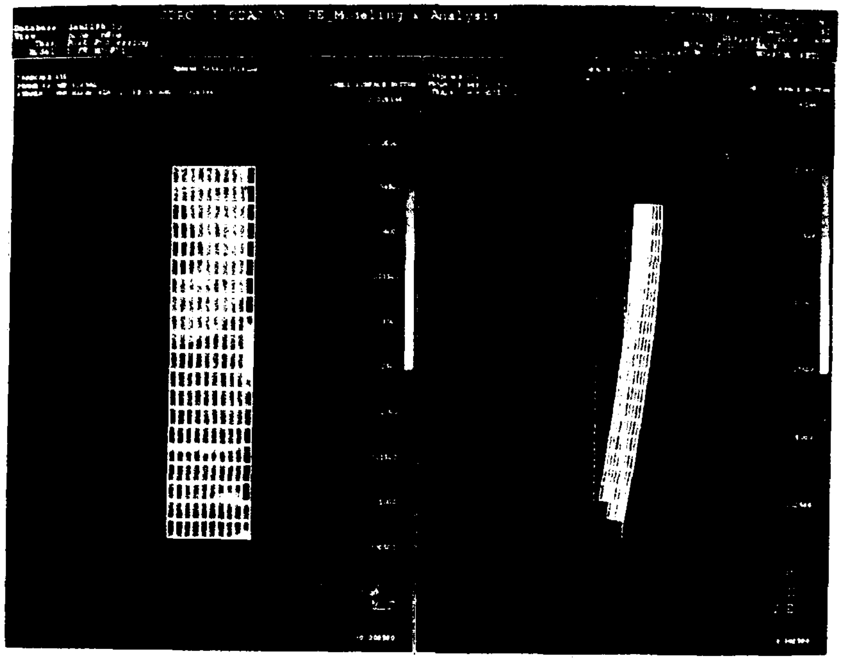

Figure B14 Levels of Von Mises strain at 27 ms

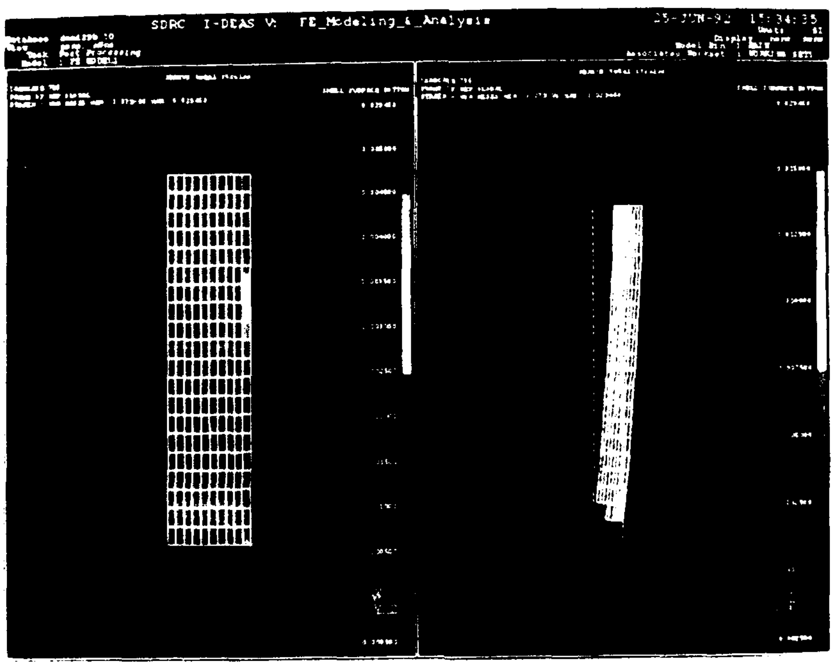

Figure B15 Levels of Von Mises strain at 3000 ms

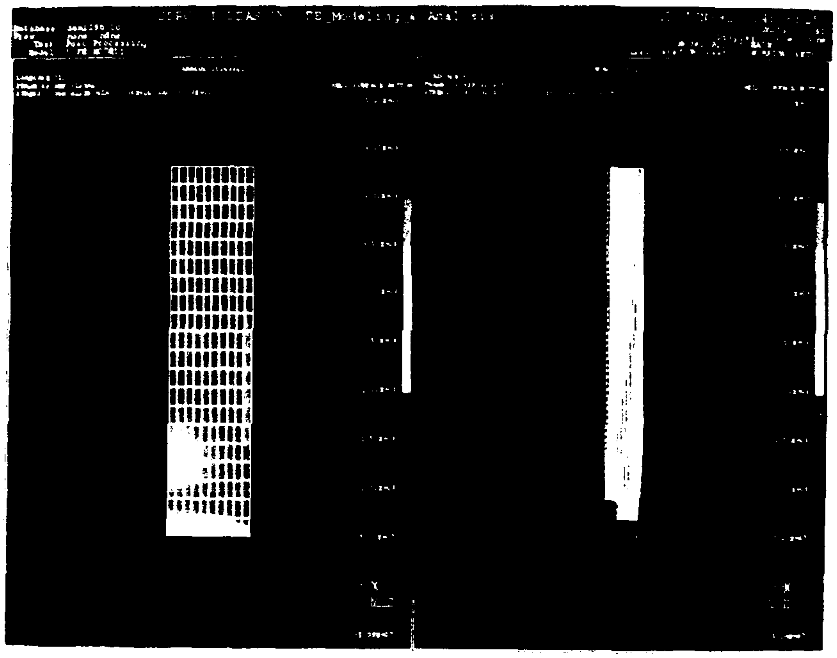

Figure B16 Levels of Von Mises' stress at 1.25 ms

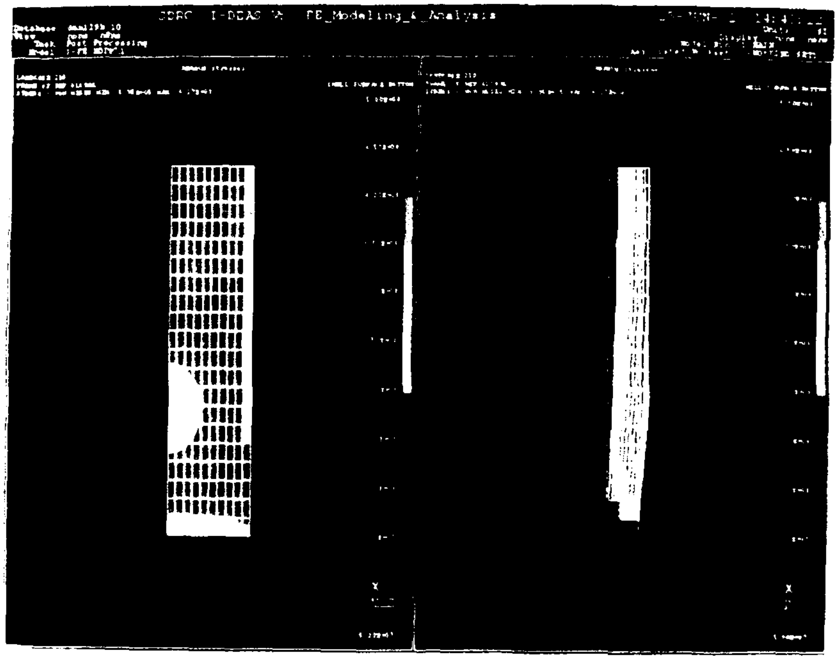

Figure B17 Levels of Von Mises' stress at 2.25 ms

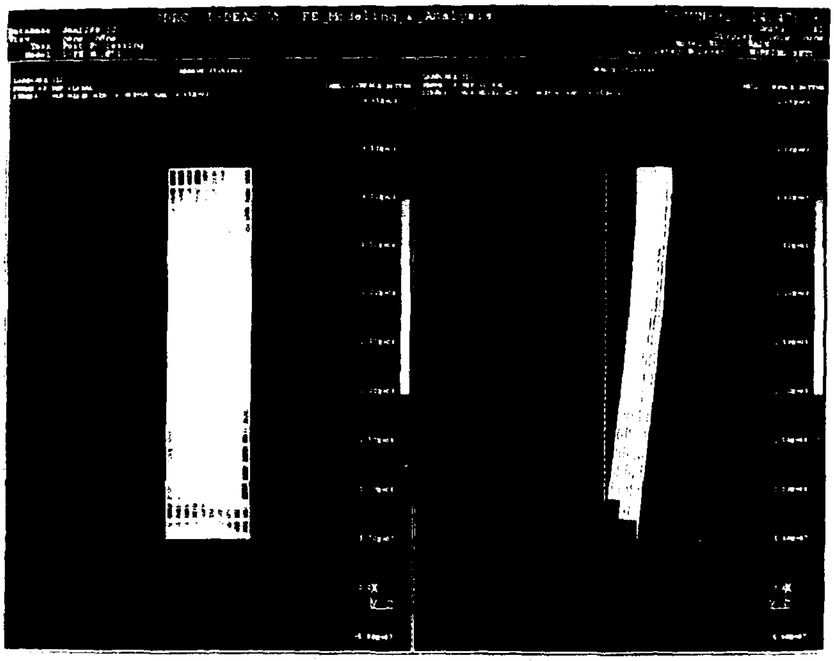

Figure B18 Levels of Von Mises' stress at 6.0 ms

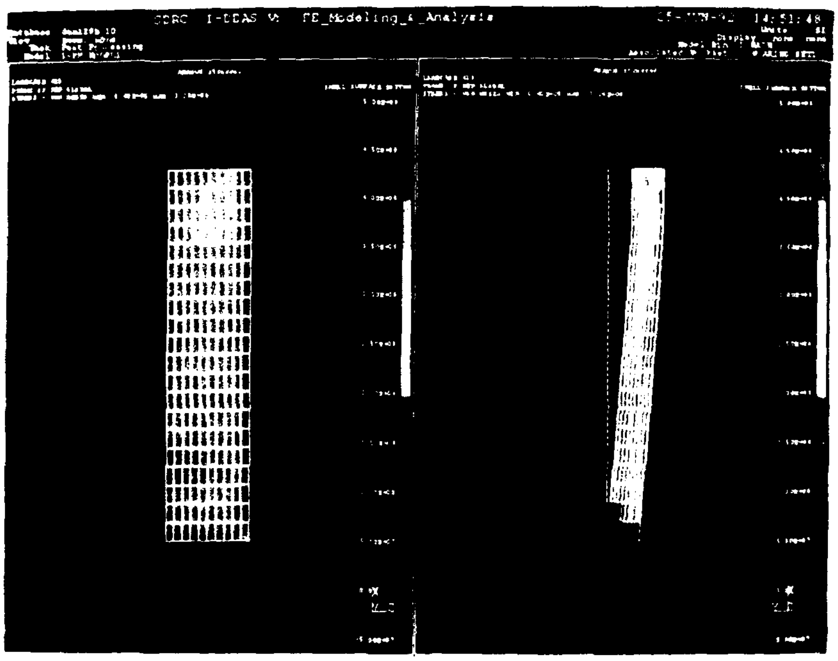

Figure B19 Levels of Von Mises' stress at 12 ms

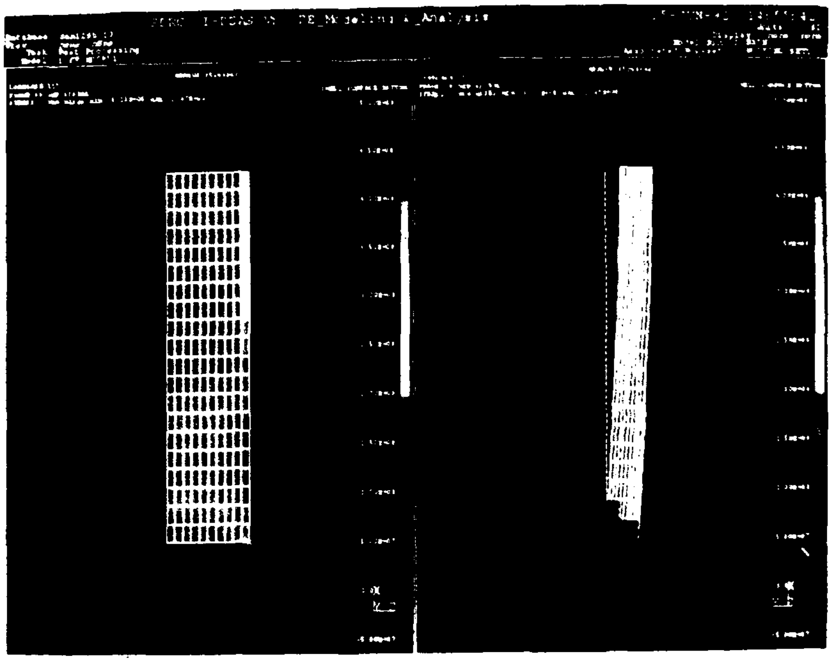

Figure B20 Levels of Von Mises' stress at 21 ms

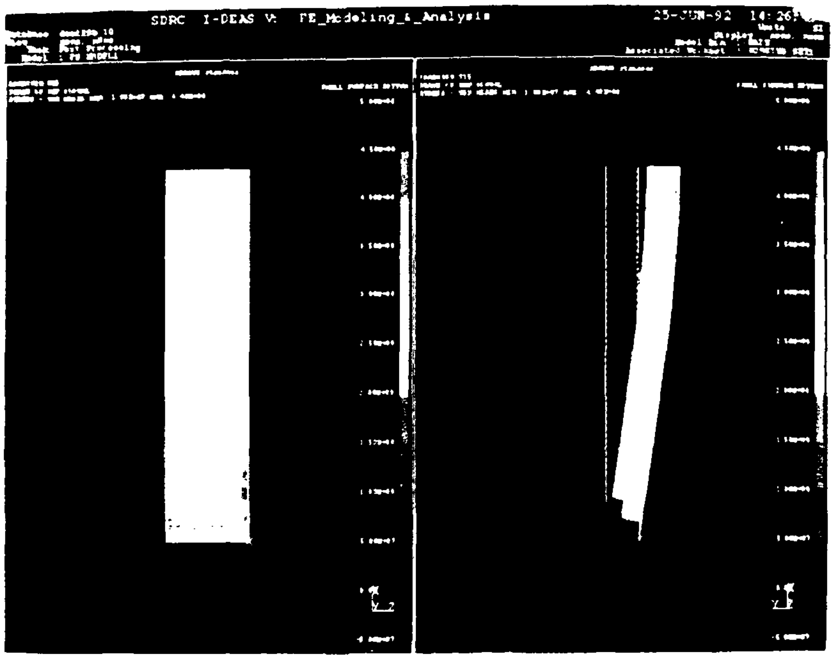

Figure B21 Levels of Von Mises' stress at 27 ms

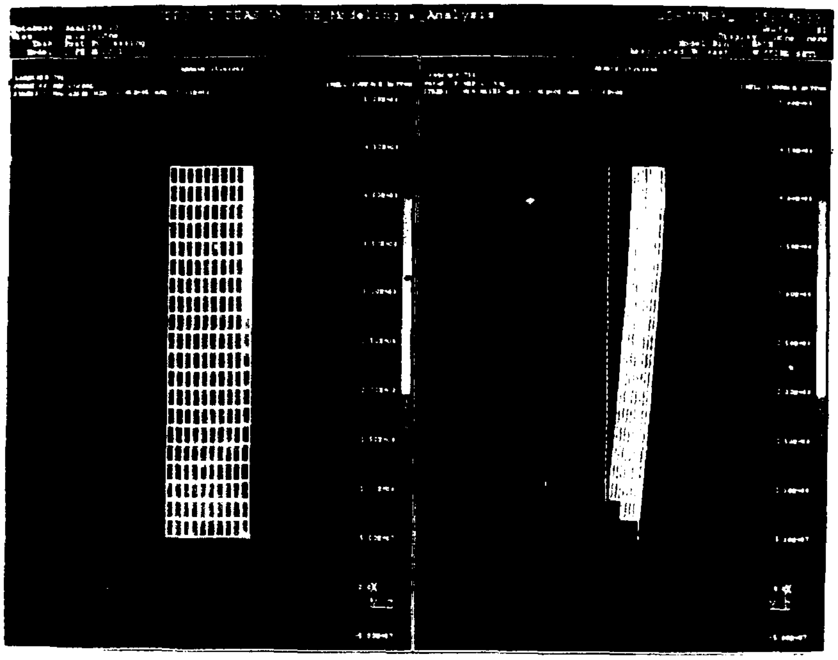

Figure B22 Levels of Von Mises' stress at 3000 ms

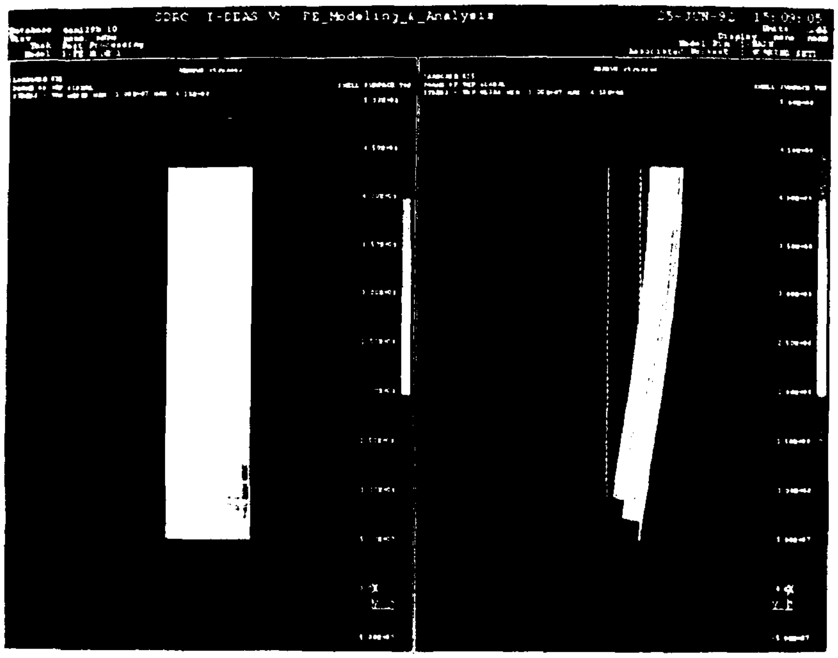

Figure B23 Levels of Von Mises' stress at 27 ms, inside

REPORT DOCUMENTATION PAGE

(MOD NL)

1 DEFENSE REPORT NUMBER (MOD-NL)	2 RECIPIENT'S ACCESSION NUMBER	3 PERFORMING ORGANIZATION REPORT NUMBER
TD92-2411		PML1992-52
4. PROJECT/TASK/WORKUNIT NO	5 CONTRACT NUMBER	6 REPORT DATE
292490195	A88/KM/419	September 1992
7. NUMBER OF PAGES	8 NUMBER OF REFERENCES	9 TYPE OF REPORT AND DATES COVERED
67 (2 Annexes)	10	Final

10 TITLE AND SUBTITLE

Validation of the internal blast response model DAMINEX with the Finite Element Method.
Progress report 1: Demonstration of the capabilities of the finite element code ABAQUS.
(Validatie van het interne blast model DAMINEX met de Eindige Elementen Methode.
Voortgangsrapport 1: Demonstratie van de mogelijkheden van de Eindige Elementen code ABAQUS.)

11 AUTHOR(S)

R.J.M. van Amelsfort
R.M.M. van Wees

12 PERFORMING ORGANIZATION NAME(S) AND ADDRESS(ES)

TNO Prins Maurits Laboratory
P.O. Box 45, 2280 AA Rijswijk, The Netherlands

13 SPONSORING AGENCY NAME(S) AND ADDRESS(ES)

Directorate of Materiel, Royal Netherlands Navy
Director of Naval Construction, Ship Research and Development
P.O. Box 20702, 2500 ES The Hague

14 SUPPLEMENTARY NOTES

The classification designation: ONGERUBRICEERD is equivalent to: UNCLASSIFIED

15 ABSTRACT (MAXIMUM 200 WORDS (1044 BYTE))

At the request of the Royal Netherlands Navy (RNLN), numerical calculations on blast-loaded ship bulk-heads were performed with the finite element code ABAQUS. These calculations are a first phase in a more extended investigation to validate and improve a simple structural response model, DAMINEX, for these panels. In this first phase, it will be demonstrated that ABAQUS is able to perform this type of calculation. This is done by simulating an ideally suited experiment: a prototype ship panel, loaded by a simulated nuclear blast. In this experiment, performed by the Canadian Defence Research Establishment Suffield, load and response are carefully measured and material properties are well analysed. Simulation results obtained with another finite element code, ADINA, are also available in the literature. The calculated ABAQUS results correspond closely with the measured results and with the ADINA results.
A second ABAQUS simulation was performed of a live-firing experiment in a decommisioned RNLN frigate. In the latter case, load, response and boundary conditions are not as well defined as in the first case. It was demonstrated that even in this situation it is possible to obtain reasonable results. So ABAQUS will be a powerful tool evaluating and improving the DAMINEX model.

16 DESCRIPTORS	IDENTIFIERS
Finite Element Methods Blast Loading Ship Bulkheads Computer Programs Computerized Simultation	Structural Response Internal Explosions

17A SECURITY CLASSIFICATION (OF REPORT)	17B SECURITY CLASSIFICATION (OF PAGE)	17C SECURITY CLASSIFICATION (OF ABSTRACT)
ONGERUBRICEERD	ONGERUBRICEERD	ONGERUBRICEERD

18 DISTRIBUTION AVAILABILITY STATEMENT	17D SECURITY CLASSIFICATION (OF TITLES)
Unlimited Distribution	ONGERUBRICEERD

Distributielijst

1	DWOO
2	HWO-KL
3/4	HWO-KLu
5	HWO-KM
6/9	DMKM-Scheepsbouw
10/12	TDCK
13	Hoofddirecteur DO-TNO
14	Lid Instituuts Advies Raad PML Prof. drs. P.J. van den Berg
15	Lid Instituuts Advies Raad PML Prof. ir. M.A.W. Scheffelaar
16	Lid Instituuts Advies Raad PML Prof. ir. H. Wittenberg
17	PML-TNO, Directeur; daarna reserve
18	PML-TNO, Directeur Programma; daarna reserve
19/23	PML-TNO, Secretariaat Divisie 2, Groep EB
24	PML-TNO, Documentatie
25	PML-TNO, Archief